Accepted Manuscript

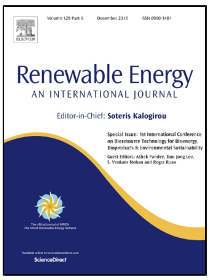

Improving spectral modification for applications in solar cells: a review

Joseph Day, S. Senthilarasu, Tapas K. Mallick

PII:	S0960-1481(18)30898-X
DOI:	10.1016/j.renene.2018.07.101
Reference:	RENE 10375
To appear in:	*Renewable Energy*
Received Date:	12 March 2018
Accepted Date:	20 July 2018

Please cite this article as: Joseph Day, S. Senthilarasu, Tapas K. Mallick, Improving spectral modification for applications in solar cells: a review, *Renewable Energy* (2018), doi: 10.1016/j.renene.2018.07.101

Improving spectral modification for applications in solar cells: a review

Joseph Day*, S. Senthilarasu, Tapas K Mallick

Environmental and Sustainability Institute, University of Exeter, Penryn Campus, Cornwall TR109FE, UK

Corresponding Author: jd553@exeter.ac.uk

Abstract

The spectral mismatch between solar cells and incident radiation is a fundamental factor limiting their efficiencies. There exist materials and luminescent processes which can modify the incident sunlight's properites to better suit the cell's optimal absorption regions. This makes for an interesting area of research and promising technique for enhancing the efficiency of solar cells which is important for environmental reasons. It is intended for this review to provide the reader with historical and up-to-date developments of the application of spectral modification to solar cells and contribute to growing its impact on real-world PV devices. We concisely outline the underlying principles of three spectral modification processes: upconversion (UC), downconversion (DC) and luminescent downshifting (LDS). For each section we present up to date experimental results for applications to a range of solar PV technologies and discuss their drawbacks. With particular focus on UC, we then review how nanostructures or integrated optics might overcome these problems. Finally, we discuss practical challenges associated with advancing this approach for commercialisation and opportunities spectral modification presents; namely where future research should focus and via a cost analysis with a simple formula that can be used to determine financial viability for the deployment of this technology.

Keywords

Downconversion, Efficiency, Luminescent Downshifting, Nanostructures, Solar Cells, Upconversion.

Contents

1. Introduction

The maximum theoretical efficiency of a 1.1 eV band gap silicon solar cell was calculated through a detailed balance model by Shockley and Queisser in 1961 to be approximately 30% [1]. However, this limit can be theoretically surpassed by the construction of solar cells in which the design and assumptions in this model need not hold true. Today there are a range of solar technologies which use new materials, going beyond traditional (or so-called 1st generation) silicon wafer based modules. These include 2nd generation thin film and 3rd generation nanostructured devices whose efficiencies and cost per watt are outlined in Table 1. Despite promising progress, if the efficiencies could be further enhanced in a non-expensive manner, then the price of solar electricity could be further reduced which would ease the transition to a sustainable global economy.

Table 1 –Various solar technologies with their maximum efficiency and cost per peak watts as of 2016. Table data from [2], [3] and [4].

Solar cell efficiency is fundamentally hampered by the following parameters [5]:

- Non-absorption of low-energy photons
- Thermalization losses from the absorption of high-energy photons
- Extraction losses due to unavoidable charge carrier recombination

In practice, optical losses [6] also occur from incomplete absorption, reflection and shading, in addition to electrical losses from parasitic series and shunt resistances [7] which further reduce the system efficiency from its theoretical maximum. However, as seen in Fig. 1, the greatest efficiency losses arise from non-absorption of high wavelength light and thermalization of short wavelength light. Collectively this problem is referred to as the spectral mismatch between the incident solar spectrum and absorption profile of the cell; it stems from a defined energy called the band gap energy, E_G, which is present in all materials that can harness solar power. Photons with $E \geq E_G$ have the potential to be absorbed and generate photocurrent; whereas photons with $E < E_G$ will be transmitted through the cell without adding to the output load. Furthermore photons of $E > E_G$ contribute to thermalization losses. This is because when absorbed they possess excess energy than required to generate photocurrent, so electrons are promoted into the conduction band with additional kinetic energy which is wasted as heat. Therefore the spectral mismatch is the key detriment to a cell's efficiency. Multi-junction or tandem cells seek to rectify this problem by combining a series of cells with varying bandgaps which are connected together either mechanically or monolithically into a single structure [8]. Through this technique, it is possible to harness a wider range of the solar spectrum, attaining higher efficiencies. In 1980 De Vos used a detailed balance model again to calculate a maximum efficiency of 68% was theoretically attainable for an infinite stack of varying band gap cells [9].

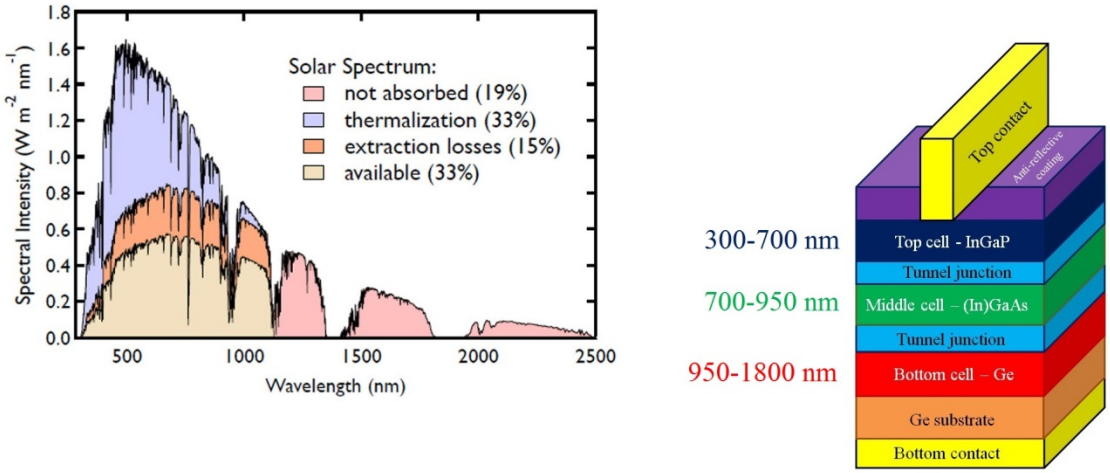

Fig. 1. The percentages of the solar spectrum represented as the energy losses that occur in a silicon cell. The spectral mismatch is responsible for approximately 50% of these through non-absorption and thermalization. The structure of an epitaxial triple junction cell and regions of the spectrum it can absorb are shown. Figures modified from [5] and [10].

In the Shockley-Queisser model it is assumed the cell only undergoes illumination by the ambient solar spectrum. From their equations, short-circuit current density increases linearly and open-circuit voltage logarithmically with the incident light concentration, hence the overall efficiency would rise under greater irradiance. According to De Vos' model a maximum efficiency of 86% is hypothetically achievable if using infinite junctions under concentrated sunlight, approaching the separately derived thermodynamic limit [11]. In reality, this means if lenses or parabolic mirrors [12] are utilized to achieve great light concentrations then higher efficiencies become possible. Also because optical materials are cheaper than semiconductor structures, a smaller area of photovoltaic surface is required which is advantageous for reducing production costs. As a result, there has been much research into and commercial deployment of concentrating solar PV technology in recent years [13]; a major challenge is maintaining a low cell temperature to maintain performance [14].

Through a combination of concentrating sunlight and multi-junction structure, remarkably efficient laboratory manufactured cells have been produced in recent years (46% in 2014 [15]). Unfortunately, these ultrahigh efficiency panels are not commercially viable for global deployment and are mainly limited to regions of the world with high direct normalized irradiance (DNI) or for use in satellites where a low weight-electrical power ratio is essential [16], so it is worth exploring alternative methods of PV cell design which surpass the Shockley-Queisser limit. One such innovative technique is to challenge the assumption that only photons with energy equal or greater than the band-gap create an electron-hole pair to generate photocurrent; so rather than modifying the materials to fit the spectrum as with tandem cells, we modify the spectrum to suit the material.

It is estimated 20% of the total photon energy in the standardised AM1.5G solar spectrum is beneath the bandgap of a monocrystalline silicon solar cell [17]. If the energy of these NIR photons could be harnessed then the amount of sunlight being converted to electricity, and hence the efficiency of the solar cell would increase. This was proposed by Wolf as early as 1960 [18] and later explored by Trupke et al [19] who calculated a maximum theoretical efficiency of 47.6% for un-concentrated sunlight and 63.2% under maximal terrestrial concentration (46,200 suns). In reality, a single photon with energy less than the band-gap *cannot* be absorbed but if the energies of two or more are combined into a single photon, through a process known as upconversion (UC), then this new quanta *can* excite electrons into the conduction band and lead to more current being produced as predicted. In practice this involves a UC layer placed beneath the solar cell to absorb transmitted radiation and re-emit it towards the cell at useful wavelengths. On the other hand, as shown by Fig. 1, an even greater portion of spectral energy is wasted via thermalization. It is also apparent solar cells give the best photovoltaic response at wavelengths closer to the band-gap of the material. Therefore, spectral modification in the opposing direction would also aid efficiency. There are two ways of producing lower energy photons from ones of higher energy; downconversion (DC) (also referred to as energy transfer by quantum cutting [20] (QC)) and luminescent downshifting (LDS). Unlike UC, it is logical to place the spectral modification material above the solar cell so a low transmittance to already optimal wavelengths is essential to result in a net gain in efficiency [21].

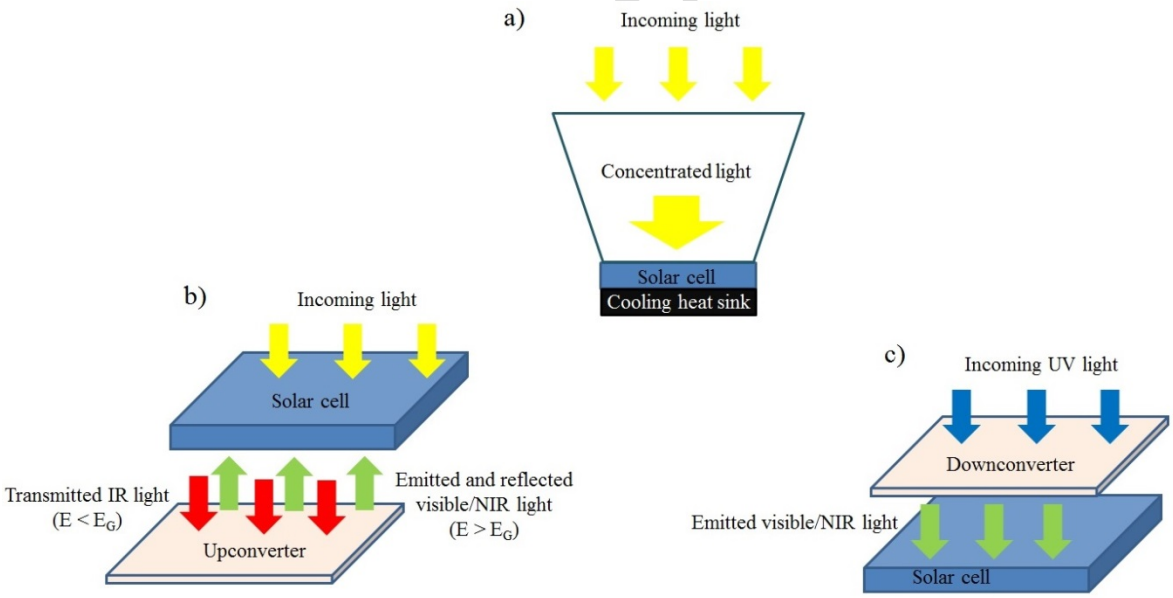

Fig. 2. The principles of: a) Concentrating PV; a lens concentrates incoming light which improves solar cell performance and reduces material demand, while a cooling sink prevents the cell from overheating. b) An upconversion layer-solar cell system. A fraction of the transmitted sub-band gap radiation undergoes upconversion and is redirected toward the cell where it is utilized. c) A downconversion layer atop a solar cell which absorbs short wavelength radiation and emits at photon energies better suited to the cell, increasing overall efficiency.

DC can be regarded as the inverse of UC. In this process a single high energy photon splits its energy between two longer wavelength photons. In 2002, Trupke et al [22] calculated a 1.1 eV band-gap solar cell's maximum theoretical efficiency could increase from 30.9% to 38.6%, following the addition of an optimal DC layer. Conversely, LDS is a process which Stokes shifts the energy of a short wavelength photon to a lower energy which is particularly useful for multi-crystalline silicon or CdTe cells with their poor responses to UV or blue light [23]. However, unlike UC and DC, LDS will not be able to supersede the Shockley-Queisser limit alone since no additional photons are generating electron-hole pairs [24]. However combining LDS materials with a concentrating geometry is an attractive route to improving cell efficiency as it can improve both the spectral response and the intensity of the incident light [25].

Many materials have been investigated for their UC, DC and LDS properties with studies predominantly focused on rare earth [26] (RE) doped lattices but also emerging alternatives such as quantum dots [27] (QDs) and organo-metallic dyes [28]. This review will present up to date investigations into spectral conversion using these materials. The limitations of these studies and possible solutions such as concentrating optics and utilising nanoscale phenomena will be discussed. Finally, we suggest where research should continue if spectral conversion is to emerge as a serious competitor to existing multijunction technology.

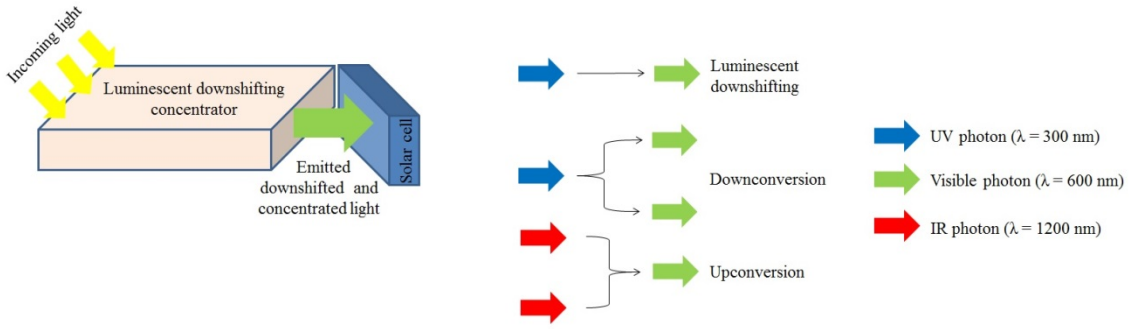

Fig. 3. Design of a luminescent concentrating PV system which both concentrates light intensity and shifts it to favourable wavelengths whilst directing it to the cell, along with a visual representation of 3 typical spectral conversion processes: UC, DC and LDS. Figure modified from [34].

2. Working principles of upconversion

2.1 Upconversion via rare earth ions

Bloembergen first suggested energy levels in transition and rare earth metal compounds could absorb IR radiation then reemit at a shorter wavelength, acting as *quantum counters* [29]. This process came to be known as *upconversion* and has been studied extensively, predominantly for applications in laser physics [30] but more recently for applications in bio imaging [31], and the focus of this review, photovoltaics. The rare earth metals in their trivalent ion state are excellent materials for UC due to their ladder-like energy structure [32] and their application to UC is the predominant scope of this review. For clarity, the term rare earth metal usually refers to elements 57-71 (the lanthanides) in addition to scandium and yttrium, but for the purposes of this paper we will use *rare earth metals* to refer exclusively to the lanthanides. Specifically, the lanthanide 3+ ions all of which have the electron configuration [Xe] $4f^n$ with n ranging from 0 to 14 [33]. It is the abundance of possible states in the 4f-orbital that allow for such a diverse range of emissions and absorptions. Although such transitions between states are parity forbidden upon doping into a host lattice, interaction with the crystal field leads to symmetry breaking and allows these transitions to take place [34]. Dieke [35] gives an excellent characterization of these states under spectroscopic notation in the so-called Dieke energy level diagrams.

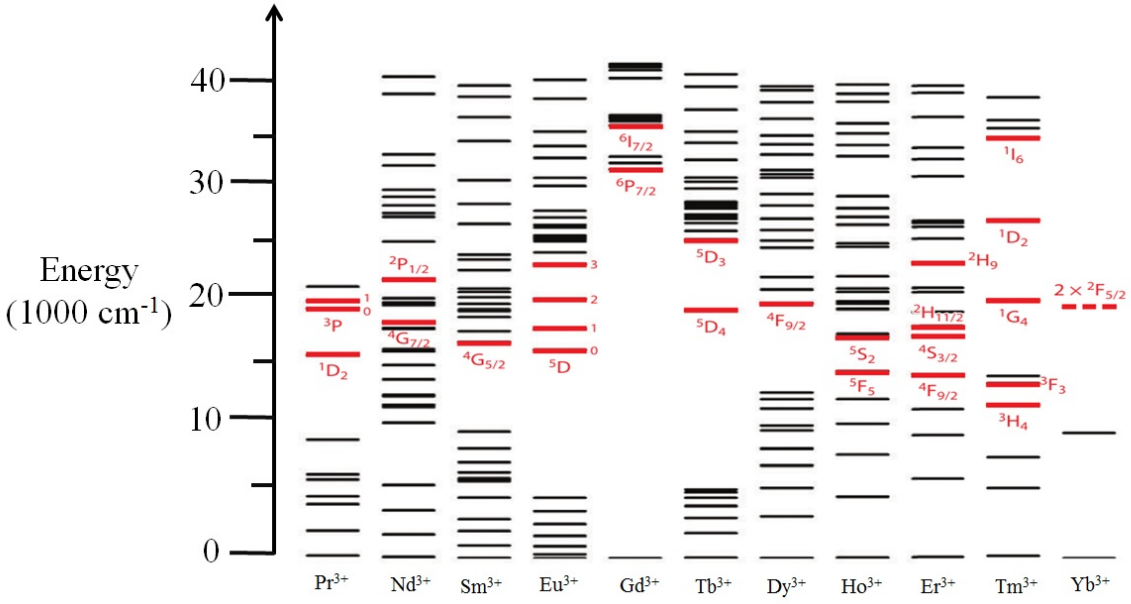

Fig. 4. A Dieke style diagram showing the energy levels of the lanthanide ions. The states highlighted in red tend to emit upconverted radiation when excited. Figure modified from [80].

There are three predominant mechanisms as described by Shalav et al which allow for photon UC in a rare earth doped compound at realistic solar concentrations [36].

- Ground State Absorption/Excited State Absorption (GSA/ESA) is a single ion process whereby an electron is promoted from the ground state to an excited state by absorbing a photon. While in this excited state a second photon is absorbed leading to an even higher energy state. When this electron relaxes radiatively to the ground state it will emit a photon of energy equal to the sum of the absorbed photons.

- Energy Transfer Upconversion (ETU) is a two ion process when nearby ions both absorb from the ground state into the excited state. One ion (the sensitizer) then transfers its energy to the other (the activator), causing the sensitizer to return to the ground state and the activator to emit a higher energy photon.

- Photon Avalanche (PA) is an unconventional UC process discovered in 1979 [37], in which energy mismatch between the incoming photon and the intermediate/ultimate excitation states leads to an exponential population of intermediate states via cross relaxation resonance.

Furthermore, in recent years two additional mechanics have been identified:

- Co-operative Energy Transfer (CET) is a three step process during which two sensitizer ions undergo excitation and transfer their energy to a single ground state activator.

- Energy Migration Upconversion (EMU) is a four step process recently proposed in 2011 by Liu et al [38] which takes place in a core-shell nanostructure and involves the interaction of 4 ions: a sensitizer, accumulator, migrator and activator.

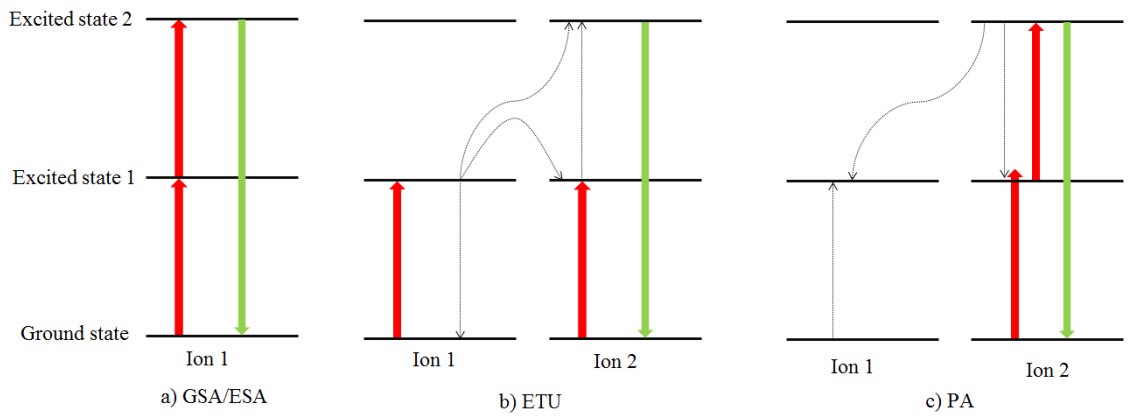

254

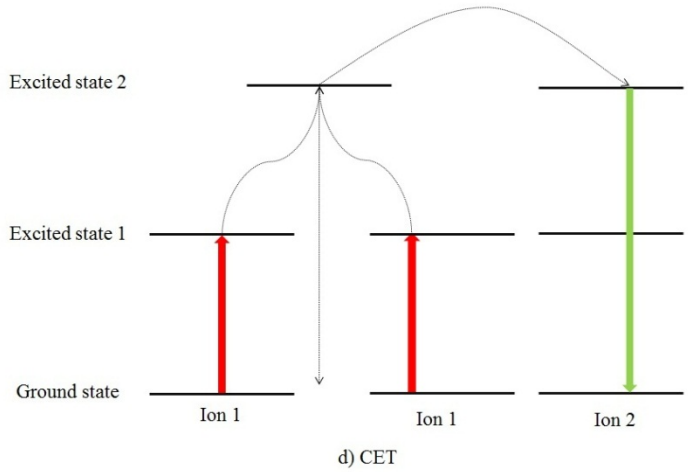

255

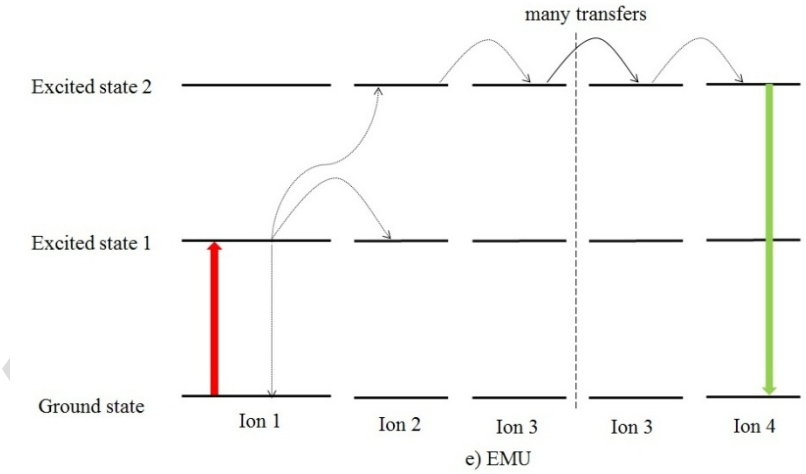

256

257 **Fig. 5. Energy diagram representation of the upconversion mechanisms in rare earth ions: a)**
258 **excited state absorption (ESA), b) energy transfer upconversion (ETU), c) photon avalanche, d)**
259 **co-operative energy transfer and e) energy migration upconversion. Figure modified from [83].**

Of these ETU is the most efficient [39] so is aimed to be the dominant process in experimental set-ups. The mechanism for a given UC material may be determined by analysing the fluorescence time decay or the pump power-luminescent intensity relation. An example of the former is demonstrated by Yang et al [40] where ESA and ETU processes were differentiated by the profile of the time decay; ESA took place during the excitation pulse and exhibited exponential behaviour (akin to direct excitation), while ETU had a longer persistence and non-exponential characteristics relating to the lifetime of the level providing energy transfer. On the other hand, Pollnau et al [41] showed UC luminescent intensity to have a dependence on absorbed pump power and in certain cases ETU and ESA could be distinguished by the measured slopes on a logarithmic plot; when n sequential photons are absorbed in a mechanism excited by pump power P, the emission intensity will show a P^n behaviour. Their theoretical results were verified with experimental investigations on four rare earth ion containing compounds. Although anomalies were found in this relationship for high-power pumping regimes which had a logarithmic slope gradient of 1, regardless of the number of steps in the mechanism [42].

Detailed state by state mechanisms presented on energy level diagrams have been proposed for specific ions, examples of which will be seen in section 3.3. However, since 2014 there have been debates in the literature about discrepancies in the frequently cited diagrams for popular UC materials and alternatives put forward. [43]. Furthermore, there have been investigations into the dependence on temperature of the ratio of UC emission from different energy states [44].

2.2 Upconversion via TTA

An alternative UC approach, utilizing organometallic compounds [45] has been suggested: triplet-triplet annihilation (TTA). The mechanism differs from the ones discussed thus far as it involves varying spin states. It could have advantages over rare earth ionic based UC due to the low excitation energies required (of the order mW/cm^2, comparable to ambient solar illumination) and the readily tuneable excitation and emission wavelengths of the sensitizers and acceptors [46]. This potential was identified by Baluschev et al [47] in 2006 following its demonstration under non-coherent solar radiation.

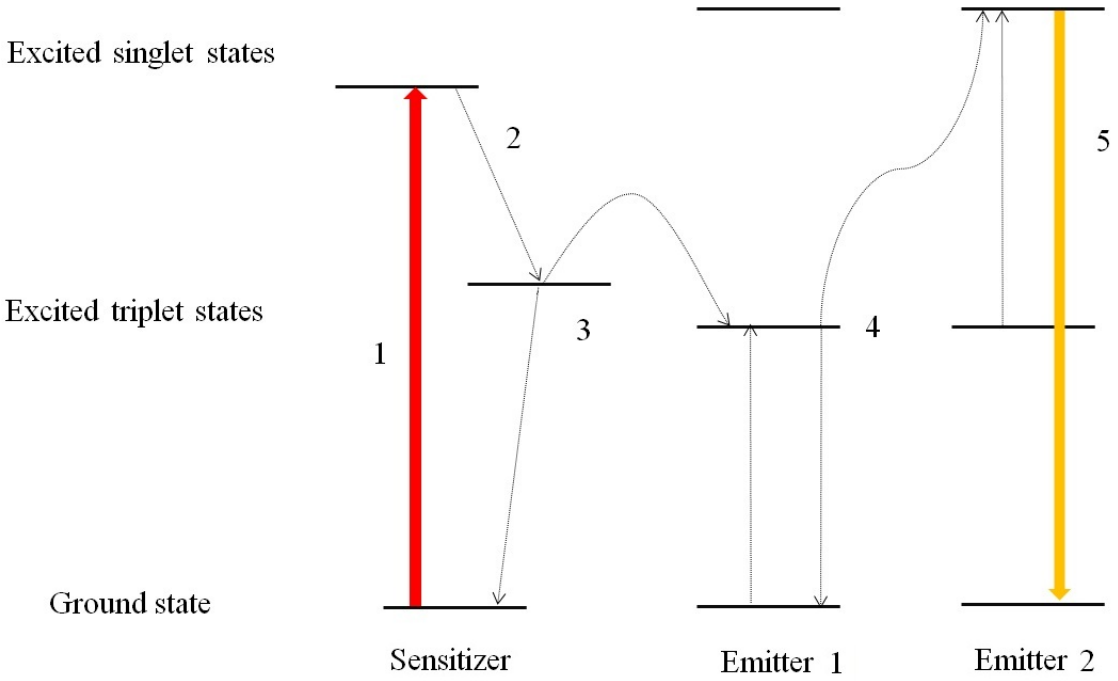

Fig. 6. The states and steps involved in photon upconversion via TTA. The numbered processes are explained in the bulk text. Figure modified from [48].

As shown in Fig. 11 this process occurs via 5 steps and is summarised by Cheng et al [48] as follows.

1. A low energy photon is absorbed by a sensitizer in the ground state.
2. Intersystem crossing (ISC) introduces the first triplet state.
3. The energy from this triplet state is transferred via a (Dexter [49]) triplet energy transfer (TET) process to a ground state emitter molecule which is excited to a triplet state.
4. TTA then occurs when two emitters in the excited triplet state undergo a *collisional complex*, yielding one in a (higher) excited singlet state and one in the ground state.
5. The excited singlet state decays, emitting a higher energy photon.

Similarly to UC via rare earth ions, this process can be evidenced by the fluorescent intensity's quadratic dependence on incident light power since TTA involves an interaction between two sensitized triplet acceptor molecules [50]. Kinetic studies by Cheng et al [51] disproved earlier assumptions in efficiency limits from spin-statistics and found the process

efficiency could reach 40%. Since the scope of this review tends towards rare earth ions, the reader is referred to [52] for a recent and in-depth report on the developments in this field.

2.3 Upconversion via quantum dots

A QD is a semiconductor nanocrystal with its excitons confined in three spatial dimensions. A fascinating attribute of QDs that make them ideal for applications in solar PV is the fact their absorption properties depend on size, so it is possible by nanoengineering to fine tune a QD to absorb radiation at specified wavelengths [53]. With these abilities, it is no surprise they have come under investigation as spectral modification materials [54-5]. Shang et al [56] in their 2015 article reviewed how QDs could be utilized for UC. Two QDs of different band-gaps are connected by a semiconductor rod. Photons are absorbed in the lower energy QD, creating an electron-hole pair. This is followed by a second photon absorption which allows the hole to tunnel to the other QD where it recombines to emit a higher energy photon. There are two ways of this occurring as shown in Fig. 12, they described two mechanisms: a) direct intraband hole absorption and b) an Auger [57] mediated process. However, unlike TTA-UC these QDs would require higher solar concentrations (by a factor of 10^5 compared to the ambient spectrum) in order to activate this kind of UC.

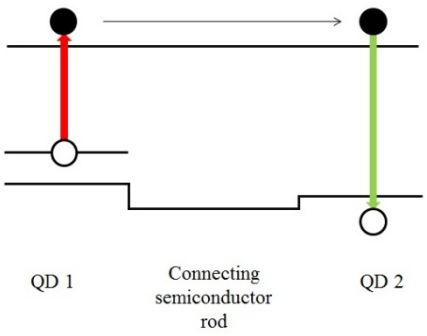

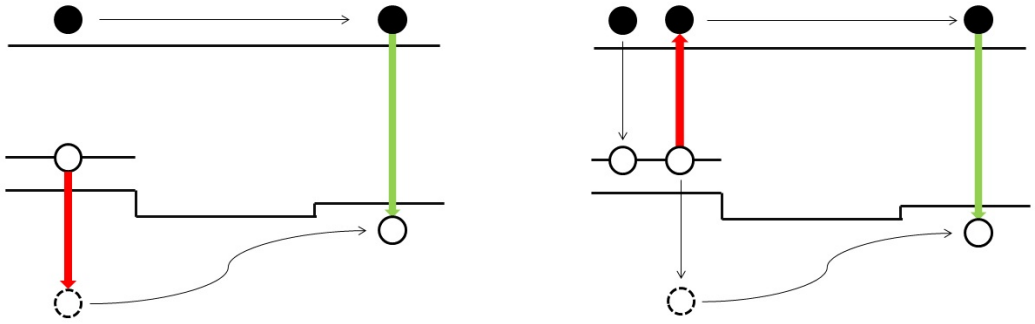

Fig. 7. Schematic of the possible upconversion processes in a quantum dot nanostructure. The overall process for QDs 1 and 2 connected by a semiconductor rod is shown foremost and can occur via two mechanisms: a) direct intraband hole absorption and b) an Auger mediated process. Figure modified from [54].

2.4 Upconversion via thermal radiation

A radically different approach to UC has been demonstrated in recent years. The underlying principle of UC via thermal radiation is to use light to raise a substance's temperature, thereby shifting its black body emission spectrum to shorter wavelengths [58] as demonstrated in Fig. 13. These emitted photons could then be utilized by a solar cell to increase efficiency. The mechanism still involves a rare-earth ion but instead of its states decaying and emitting photons, the energy is absorbed into the lattice producing heat.

3. Upconversion experiments

3.1 Early experiments

Initially, Impurity Photovoltaic (IPV) devices were envisaged that would dope metal ions directly into the cell substrate and through their energy levels allow IR light to undergo UC and generate additional electron-hole pairs [59]. Yet in 1996 Gibart et al [60] found the efficiency of a GaAs cell to be 2.5% under 891 nm illumination (less photon energy than the cell GaAs bandgap), when a 100 µm thick vitroceramic containing Er^{3+} and Yb^{3+} ions was applied to the rear of the cell. This first ever proof-of principle experiment showed UC could utilise sub band gap photons in a solar cell. It has since been accepted separate up converting

layers have more potential over IPV as they can be materially optimised independently from the cell [61] and in early experiments on silicon, the additional layer outperformed IPV cells [62].

Rare earth metals were identified as the leading up converting materials in this field and Auzel gives an excellent review of the mechanisms responsible [63] in more detail than outlined in the previous section. In the years following, there have been many more proof-of principle experiments demonstrating UC to be beneficial to the efficiency of many types of solar cell (see Appendix 1). However, despite the growing interest and performances in UC devices, the area faces many challenges. Even the best results have only led to modest increases in efficiency. This is primarily due to the low quantum yield of the UC process and narrow absorption bands of the rare earth metals [64]. Thus, we present in the later sections of this review paper, innovative techniques, experimental data and where to go next if we are to make the process more efficient, which is necessary if it is to become a viable technology for commercial solar cells.

3.2 Upconversion efficiency and its limitations

When quantifying the efficiency of UC processes, several values are quoted. Frequently presented are the internal or external photoluminescent quantum yields (*iPLQYs/ePLQYs*), which are sometimes referred to as UCQY. These are defined as the fraction of absorbed or incident photons emitted at the UC wavelength, so that:

$$iPLQY = \frac{number\ of\ photons\ emitted}{number\ of\ photons\ absorbed} \qquad \text{(Equation 1)}$$

$$ePLQY = \frac{number\ of\ photons\ emitted}{number\ of\ incident\ photons} \qquad \text{(Equation 2)}$$

Therefore, an *ePLQY* of 50% would imply a perfect absorption and two low-energy photons to one high energy photon process. These values can be measured experimentally by using an integrating sphere [65]. If an upconverter is combined with a solar cell the overall external quantum efficiency (*EQE*) of the system is given by:

$$EQE = \frac{number\ of\ electron\ hole\ paris\ generated}{number\ of\ incident\ photons} \qquad \text{(Equation 3)}$$

Studies had until recently predominantly focused on monochromatic illumination of UC materials with speculation for PV applications. However, as the field has developed, there have been more reported physical PV-UC systems having their power conversion efficiency (PCE) and short-circuit current density (J_{SC}) measured under a solar simulator. Furthermore, in phosphor luminescence studies it is common to quote the normalized EQE (*NEQE)* measured in cm^2 / W and defined as:

$$NEQE = \frac{EQE}{incident\ light\ power\ density} \qquad \text{(Equation 4)}$$

Although one should be careful when contrasting these values, since UC is a non-linear process [66] so quantum efficiency is not independent from incident light concentration. The iPLQY follows a power law:

$$iPLQY \propto P_{in}^{n} \qquad \text{(Equation 5)}$$

P_{in} is the incident power and n the number of steps in the UC mechanism. On the other hand, the EQE of single junction solar cells has a linear relationship with increasing intensity. Combining the two processes for a UC-PV system we see the overall EQE in response to sub-band gap illumination scales:

$$EQE \propto \frac{P_{in}^{n}}{P_{in}} \propto P_{in}^{(n-1)} \qquad \text{(Equation 6)}$$

So for a predominantly ETU process which has two steps, the EQE is expected to scale linearly with increased radiation. This law holds at low irradiance but at higher irradiance deviates from theoretical value due to competing processes [67]. Therefore, if a higher concentration of light on the upconverter can be achieved the PV efficiency rise will be greater.

Shalav et al identified three dominant losses that depopulate the excited states [68]. Collectively these processes are known as quenching. Firstly, multi-phonon transitions are a type of non-radiative relaxation to lower energy states; if more than six phonons are required then radiative relaxation will dominate [69]. Hence it is essential to use low phonon energy hosts such as halides [70] when designing compounds for UC experiments. Secondly, radiative relaxation can occur, resulting in the emission of a photon of lower energy than desired. And finally, energy transfer called cross-relaxation can take place between ions, leading to unwanted low energy photon emission. This is particularly prevalent for high rare-earth doping concentrations [71], so the ratios should be carefully selected.

Since the UC process is the transfer of energy between states in a material, it can be modelled by simulations. The fundamental dynamics of a luminescent body are underpinned by the following rate equation [72]:

$$\frac{dN}{dt} = -(A_r + A_{nr})N \qquad \text{(Equation 7)}$$

Where N is the population of excited states and A_r and A_{nr} are the radiative and non-radiative decay rates. From this equation one can see in the absence of illumination the excited population decays exponentially with time constant [73]:

$$\tau = \frac{1}{A_r + A_{nr}} \qquad \text{(Equation 8)}$$

The quantum efficiency of the photoluminescence is simply the ratio of radiative decay to total decay [74]:

$$\eta = \frac{A_r}{A_r + A_{nr}} = \frac{\tau_r}{\tau} \qquad \text{(Equation 9)}$$

So the quantum efficiency can be calculated by comparing observed lifetimes to τ_r which can be estimated from Judd-Ofelt theory [75]. Furthermore, empirical observations into non-radiative decay rates have shown the so called "energy gap law" [76]:

$$A_{nr} = A_{nr}(0)e^{-\alpha(\Delta E)} \qquad \text{(Equation 10)}$$

In this law, A_{nr} *(0)* and α are constants that depend on the host lattice and ΔE the gap in energy between the states. This re-iterates the need for low phonon-energy host lattices since a large energy gap will require more phonons to bridge, hence the exponentially decaying decay rate. With these equations (and more complex quantum mechanics if required) it is possible to model up conversion processes in rare earth doped lattices with a range of energy levels. These simulations can then be compared to experimental data. In 2012 Fischer et al [77] demonstrated this by modelling the transition probabilities in 20% Er^{3+} doped $NaYF_4$ and consistency with observed data meant using rate equations to simulate behaviour was physically reasonable. Shyichuk et al [78] extensively analysed ETU dynamics in YVO_4:Yb^{3+}, Er^{3+}. A set of rate equations was compiled and solved numerically using the Runge-Kutta method. Agreement with experiment showed they were successfully able to predict the macroscopic properties and dynamics of the system from microscopic considerations of the Er^{3+} ions' behaviour. Their new methodology is advantageous to prior theoretical models as it can be generalised to any crystal matrix with known structure and various experimental illumination set ups. These studies increase our understanding of the fundamental behaviour in a UC material, so its development is a necessary task if we are to produce a highly efficient upconverter.

3.3 Rare earth ions used for upconversion

Of the rare earth ions, Er^{3+} has stood out as an excellent candidate and has been widely tested for UC. This is because it has a suitable absorption spectrum centred at 1523 nm, with emission lines predominantly at 980nm, resulting from the $I_{11/2}$ to $I_{15/2}$ transition [79]. These values are remarkable for PV applications since 1523nm is an intense region of IR radiation in the sea level solar spectrum (25W/m^2) and a photon of wavelength 980nm has energy close to the band gap of a crystalline silicon solar cell (c-Si). Yb^{3+} - Er^{3+} co-doped lattices have too shown excellent potential. Yb^{3+} has a larger cross-section than most ions (9.11 x 10^{-21} cm^{-2} at

976 nm for the $^2F_{7/2}$ to $^2F_{5/2}$ transition) [80] and can act as an excellent sensitizer to another rare earth ion. These UC materials have higher UCQYs with approximately 50% of absorbed NIR photons emitted in the visible range [81]. The absorption and emission spectra of Yb^{3+} - Er^{3+} co-doped compounds are better suited for applications in wide band-gap PV, such as amorphous silicon or perovskite cells. The absorption peak for Yb^{3+} - Er^{3+} is located at 980 nm, with emission across the 400-700nm range [82]. Additional rare earth metals have potential across the required wavelengths. In their 2013 review Huang et al [83] classify all possible transitions with relevance for spectral conversion in solar PV. However, Er^{3+} and Yb^{3+} - Er^{3+} aside, their frequency in the literature of being applied to solar cells is sparse.

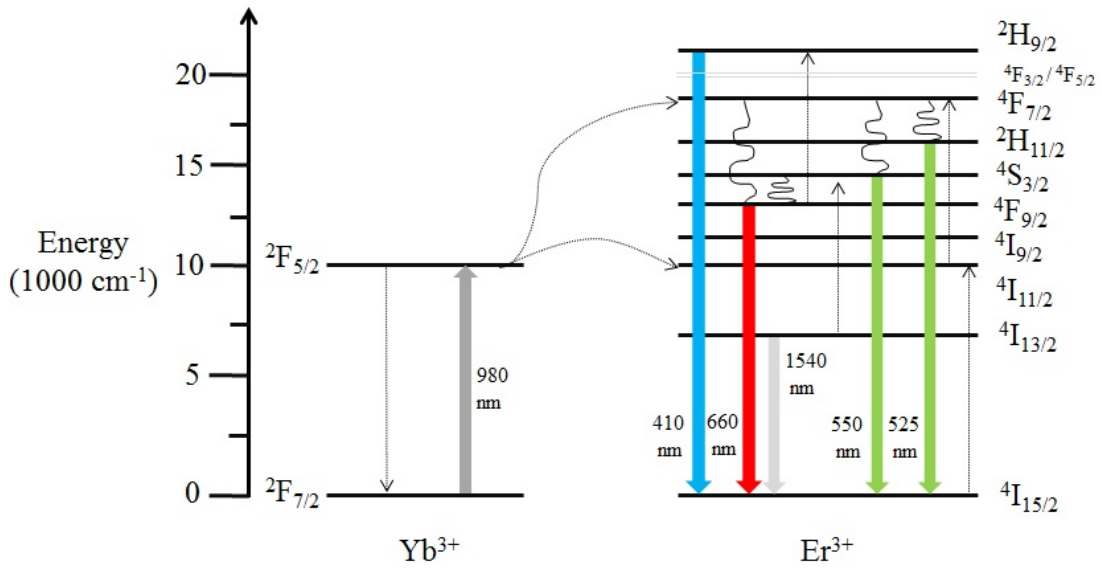

Fig. 8. Energy level diagram showing the possible emissions from the Yb^{3+}-Er^{3+} ion pair. The dashed lines represent energy transfer, the solid lines radiative decay and the curly lines non-radiative decay. Figure modified from [81].

Dy^{3+} has a similar energy level structure to Er^{3+}, so has theoretical potential for UC in solar cells. Er^{3+} - Dy^{3+} co-doped lattices can absorb at 1300nm and emit at visible wavelengths, but investigations showed improved UC efficiency was needed to match the emission intensity as compared to 1.5µm excitation [84]. Likewise, Tm^{3+} ions absorb at 1220nm and emit at 808nm. Rodríguez-Rodríguez et al [85] analysed UC in Tm^{3+} doped glasses for applications in PV yet they estimated only an additional EQE of 0.1% was attainable at high solar concentrations. This negligible improvement meant the authors concluded its use unlikely to be justified in solar cells. However, the Ho^{3+} ion does appear more promising. It has a wide absorption in the 1150-1225nm range [86]; this part of the ambient solar spectrum is approximately twice as intense as at the 1530nm centred Er^{3+} absorption. Ho^{3+} doped fluoroindate glasses have been successfully tested for efficient UC and excitingly they are

transparent at 1540 nm. This is significant because it means there is potential for a multi-wavelength UC device containing a Ho^{3+} layer atop an Er^{3+} layer, which allows for photon UC occurring simultaneously in the two biggest regions of the sub band-gap spectrum. This design was conceptualised by Lahoz et al [87] in 2011 but to this author's knowledge, no such device has been assembled and tested on a solar cell as of December 2016.

3.4 Synthesis of upconversion materials

When choosing UC materials, a host lattice with a low phonon energy and high chemical stability is of most importance, with Sun et al [88] identifying ideal compounds as REF_3, REOF or $MREF_n$ (M = Li, Na, K, Ba; n = 4, 5). Thus unsurprisingly one of the most popular host lattices for doping Er^{3+} has been $NaYF_4$ with widely reproduced syntheses originating from Kramer's group in 2004 [89]. There are two occurring phase structures of NaYF4; cubic α-NaYF4 and hexagonal β-$NaYF_4$. Of these the hexagonal β-phase has a much greater potential for UC devices as its emission has been shown to be comparably greater than the α-phase [90]. Hence it is crucial in the synthesis to ensure cubic impurities are kept to a minimum. Also it is important to carefully select the doping concentration of the rare earth ion. Too much causes cross-relaxation processes to dominate, leading to low UC efficiency; too little and large distances between the rare earth ions results in a low energy transfer rate and similarly poor yield [91]. It's therefore desirable to strike a balance between these extremes. A further practical consideration for applications to PV cells is that the rare earth doped compounds exist in powder form, so a chemical etchant is required to act as a host matrix and allow for construction of a real-world system. Polyfluorocyclobutane (PFCB) has been a popular choice for its transparency to NIR radiation and similar refractive index to $NaYF_4$ in order to reduce scattering [92]. These properties are vital to not incur further optical losses. Thus, when preparing UC materials, it is important to use the ideal doping concentrations and ratio of UC compound to host matrix. Ivaturi et al [93] explored thoroughly the effects of varying Er^{3+} doping concentrations in a $NaYF_4$ lattice and phosphor-PFCB matrix mass ratio. They found the optimum Er^{3+} doping level to be 25% and phosphor concentration in the matrix to be 84.9 w/w %. Despite these fundamental losses, there are other sources of inefficiency that arise when building a practical UC device. Boccolini et al [94] have argued that losses occur due to re-absorption in a UC layer, so optimizing the thickness is essential for an efficient process. Using simulations, they were able to show the thicknesses that yielded the greater intensities of up converted light.

Alternative materials seek to improve the efficiency increase by obtaining a higher up conversion quantum yield. Fluoride glasses such as ZBLAN (which contains fluorides of Zr, Ba, Ln Al and Na) have been doped with Er^{3+}, reaching an impressive 12.7% absolute up conversion efficiency [95]. Other emerging host lattices for this Er^{3+} transition, have included 30% doped BaY_2F_8 and 10% doped Gd_2O_2S, which reached eUCQYs of 9.5% and 12% respectively [96-97]. The use broadband as opposed to monochromatic illumination also provides higher quantum yields and is more like the ambient solar spectrum which is relevant for real world systems. Goldschmidt et al speculated that the higher yields arise from a broader incident spectrum containing more photons at resonant wavelengths for the intermediate transitions in a UC process [98]. MacDougall et al [99] first investigated the

effect of broadband illumination on the UCQY of 10% Er^{3+} doped $NaYF_4$. They found the iUCQY to increase from 8.7% to 16.2% upon widening the bandwidth from 12 to 61nm. Then Arnaoutakis et al [100] prepared a UC structure to the specifications recommended by Ivaturi et al [101]. Using a quartz tungsten halogen lamp and relevant filters, they illuminated the sample under various broadband excitations. Again it was demonstrated that the wider incoming spectrum (1400-1600nm) produced the highest iUCQY of 4.27%, compared to 1.61% at 1500-1550nm.

3.5 Upconversion applications for silicon PV

In an early significant study, Shalav-et al [102] placed a planar bi-facial c-Si cell above a 20% Er^{3+} doped $NaYF_4$ UC layer. This set up was illuminated by a 6mW 1523 nm laser and a maximum EQE of 3.4% was measured, however the cell performed poorly under lower intensity illumination (only a few times better than an IPV Er^{3+} doped cell). The group had also prepared Tm^{3+} and Ho^{3+} doped $NaYF_4$ phosphors but unfortunately were unable to characterise them due to the intense light required. The authors calculated an overall maximum theoretical efficiency increase of 2.4% absolute and recommended a much broader absorption spectrum was needed if this approach was to have an impact on commercial solar cell production. Following this group's work, more UC layers have been applied to solar cells and had their efficiencies measured, including under broadband excitation. In 2011 Goldschmidt et al [103] applied 20% Er^{3+} doped $NaYF_4$ to a silicon solar cell and under 1460-1600 nm radiation, the UC efficiency was 1.03% which under ambient solar incidence would lead to a relative efficiency increase of 0.014% (the cell's regular efficiency was 16.7%). Again it was concluded this was too low to have an immediate significant impact. However, by 2013, a potential relative efficiency increase of 0.16% was found via short circuit current density measurements; 4.03 mA/cm^2 on a silicon cell that had been applied with 25% Er^{3+} doped NaYF4 under 1450-1600nm illumination [104]. The group had also found a novel way to calculate relative solar concentrations for broadband spectral mismatches at given wavelengths, useful for UC applied to concentrating PV Results from 2015 show further progress; 30% Er^{3+} doped BaY_2F_8 achieved an extra short-circuit current density of (17.2 ± 3.0) mA/cm^2. This represents a relative enhancement of the short circuit current of (0.55 ± 0.14) %, 35-times higher than values published in 2011 [105].

Other types of silicon cells have too been tested for UC. A significant increase in efficiency of a multi-crystalline silicon solar cell (mc-Si) was reported in 2011 by Chen et al [106]. $La_2Mo_2O_9$ was co-doped with Yb^{3+} - Er^{3+} or Yb^{3+} - Ho^{3+}. Against precedent, they placed the UC layers on top of the cell, but this was able to reduce reflectance losses and in fact increased the cell efficiency by 1.5-2.7% relatively despite a low UC process performance. A widely studied class of thin film solar cells are those based on amorphous silicon (often abbreviated to a-Si or a-Si:H if undergone hydrogenation). These cells have the advantage that they require far less material than traditional wafer-based crystalline cells which leads to a lower energy payback time [107]. Also UC devices were predicted by Atre and Dionne to be of more use to thin film technologies due to their wider band gap (meaning a greater portion of the solar spectrum's photons lie below the band gap) [108]. In 2010 de Wild et al [109] reported a 0.01 mA/cm^2 short-circuit current density on an amorphous silicon solar cell

under 980nm illumination that had had β-$NaYF_4$ doped with 18% Yb^{3+} and 2% Er^{3+} applied to the rear. This represented only a slight increase from the background short-circuit current of 5μA/cm^2. However, sources of loss were discussed and efficiency improvement suggestions made. A major drawback was identified as the poor response of the cell to rear-side illumination following UC. In a recent study Qu et al [110] prepared rare earth co-doped β-$NaYF_4$ phosphors with different combinations: 20% Yb^{3+} - 1 % Er^{3+}, 25% Yb^{3+} - 1 % Ho^{3+} and 60% Yb^{3+} - 0.5 % Tm^{3+}. The Er^{3+} doped performed best increasing overall efficiency by 7.3% relative whilst also providing an improved scattering function. Furthermore in 2015, Chen et al [111] observed a remarkable improvement over $NaYF_4$ by studying 28% Er^{3+} doped $BaCl_2$. Unlike previous studies these ions were excited at two distinct wavelengths (980 and 808 nm). They found upon broadband excitation >800nm its emission at 410-667 nm was substantially more intense with great potential for enhancing the efficiency of a-Si: H solar cells. In a later publication [112] the same group stated under non-coherent NIR simulated sunlight the photo response of an a-Si:H cell greatly enhanced to 0.6 mA/cm^2. Moreover tri-wavelength simultaneous excitation at 1530, 980 and 808 nm has been observed through an Er^{3+} doped LaF_3 embedded oxyfluoride glass ceramic applied to an a-Si:H cell [113].

3.5.1 Enhanced upconversion via concentrating PV

Recalling the non-linear nature of the UC process, a conceptual design for a spectral and geometric concentrator up converting system was proposed by Goldschmidt et al in 2008. They predicted their specifications could raise the conversion efficiency of a bifacial solar cell from 23% to 25% [114]. Fischer et al used a Fresnel lens under a solar simulator to concentrate light onto an Er^{3+} doped $NaYF_4$ layer beneath a bifacial solar cell. At a level of 210 suns the short-circuit current increased by 13.1 mA/cm^2, corresponding to a relative efficiency increase of 0.19% [115]. A further complication arises because the optimal solar concentration for the cell will differ to the ideal conditions for the spectral conversion layer. Some groups have investigated this imbalance and constructed integrated optics-solar PV systems to compensate for the difference in concentration levels. Optical fibres combined with dielectric tapers [116] have been investigated as components that can increase light concentration to 2000 suns at specific wavelengths for PV applications. This integrated optics approach has been tested to look for an increase in photo response in a UC-PV device under sub-band gap illumination [117] and results showed the concentration on the UC layer can be independently optimized regardless of the intensity at the cell's surface (an important step forward for UC's potential in CPV). Arnaoutakis et al [118] demonstrated this by designing such a device which placed a compound parabolic concentrator between a bifacial silicon solar cell and up conversion layer as shown in Fig. 15. The group observed an increase in the cell's EQE of 1.80% with the integrated system as opposed to 1.33% with the non-integrated up conversion layer. Fischer et al [119] have investigated the relation between excitation power density and Er^{3+} doping level in the successful lattices $NaYF_4$ and Gd_2O_2S. Using simple models, they determined the optimum doping level decreases as the illumination increases. This is something for groups to bear in mind when preparing UC materials for use in set-ups of varying concentration.

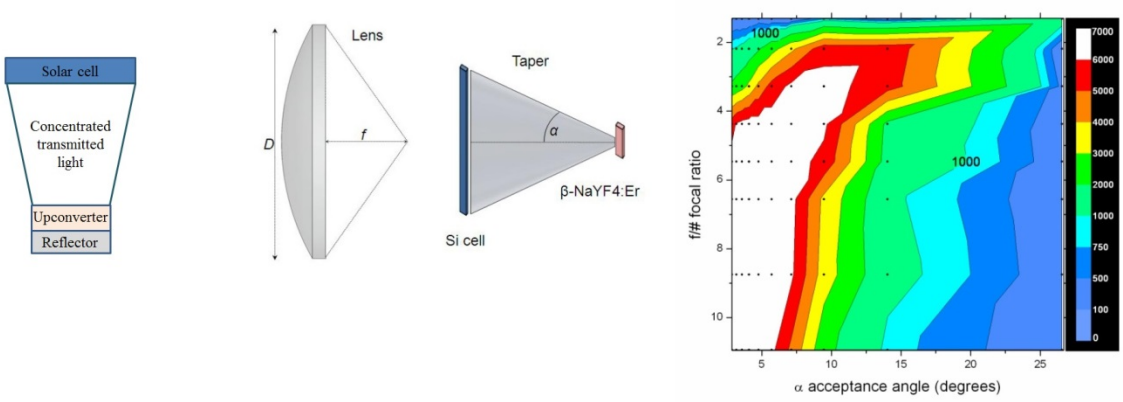

Fig. 9. A hypothetical cross-section of a UC-PV system with an array of compound parabolic concentrators between the layers., along with the schematic of a system modelled by changing parameters α and focal ratio (f/D). High concentrations >1000X may be achieved. Figure modified from [120] and taken from [79].

Geometric optical modelling has also been applied to concentrating UC systems to optimise set up for maximum concentration of light. Ray-tracing optics and Monte Carlo [120] simulations often form the bases of these investigations. Arnaoutakis et al [121] modelled the optical system shown in Fig. 17 to determine the geometric concentration of light at the UC sample. It was found to reach 6000X for acceptance angles below 10º and f/# greater than 3. If such an intense beam could be configured it would result in a much higher quantum yield of the UC layer.

3.5.2 Enhanced upconversion via thermal radiation

In 2014 Wang et al [122] showed UC with an efficiency of 16% could be achieved by thermal radiation. Yb^{3+} doped ZrO_2 was the material of choice for its high melting point, high thermal conductivity and strong infrared absorption. In juxtaposition to conventional UC host lattices, multi-phonon relaxation becomes a *desirable* process since incoming radiation needs to be dissipated as heat to the crystal. The oxide powder was heated to 2850K under a 976 nm, 570 W/cm^2 laser and Wien's displacement law and conduction loss considerations used to give the efficiency. Further investigations used concentrated white-light to test if this glowing could be harnessed to improve solar cell efficiency. It was also compared to the widely used Er^{3+} doped $NaYF_4$ and found to perform worse at low excitation powers but better at high concentrations. Practical considerations when designing such a system must be to thermally isolate the solar cell from the radiation source, as from solar cell and semiconductor theory allowing the temperature to increase would have a detriment on its performance. Geometrical arrangements are briefly discussed whereby it is assumed a lens beneath a bifacial solar cell would concentrate transmitted photons, focus them onto a thermal UC material then redirect its radiation back towards the cell. Boriskina and Chen

[123] further developed a conceptual thermal UC-PV platform. Angular selectivity could be realised by nanomaterials or a reflective cavity with small aperture. It was envisaged to achieve a 73% maximum up conversion efficiency and a limiting silicon PV cell efficiency of 45%, surpassing the Shockley-Queisser limit. In 2015 Chen et al [124] tested thermal UC in a $CeVO_4$ powder over the range 808-1064 nm in a system with an amorphous silicon solar cell. Upon sub band-gap illumination photocurrents of order 1 mA/cm^2 were observed, demonstrating "colossal" potential for wide band-gap solar cells.

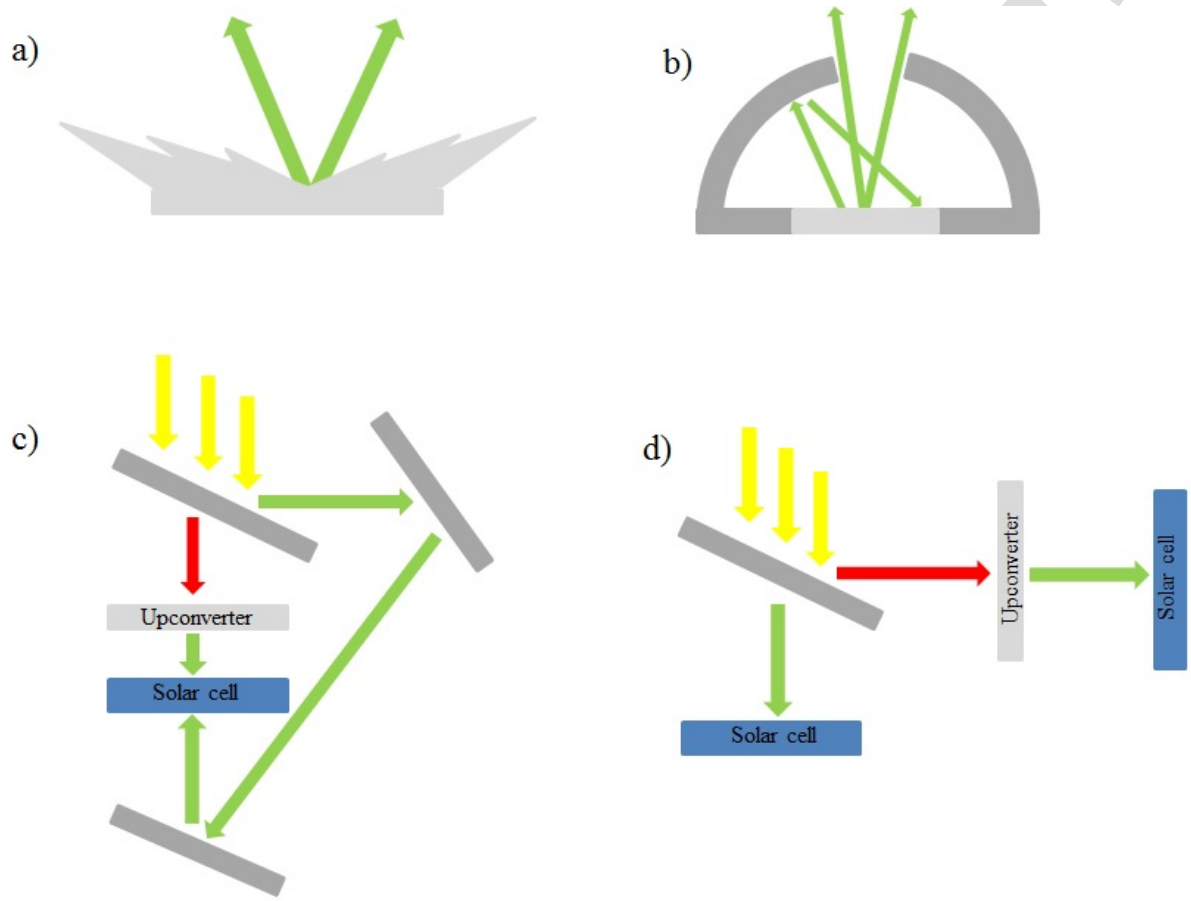

Fig. 10. Schematics of possible physical UC via thermal radiation systems: a) angular selectivity by surface nano-patterning, b) enclosing the upconverter into a reflective cavity with small aperture, c) geometrical and spectral splitting of sunlight onto a cell d) same concept as c) but with two cells. Figure modified from [124].

3.6 Upconversion applications for emerging PV

3.6.1 Dye Sensitized Solar Cells

Dye Sensitized Solar Cells (DSSCs) were proposed in the 1980s and first realised by Grätzel in 1991 [125]. These cells also have the advantage of being lightweight and cheap to produce so even if efficiencies are relatively low, they may economically compete with well-established technologies if improvements in stability can be implemented [126]. The most commonly used dyes are ruthenium-based containing carboxyl groups (such as N-719 [127]) that absorb poorly beyond 700nm, so a UC enhancement would allow more of the spectrum to be utilized by the dye, generating more current and higher cell efficiency.

Shan and Demopoulos [128] first attempted to increase DSSC efficiency this way adding Yb^{3+}-Er^{3+} co-coped LaF_3 into the TiO_2. Unfortunately, although the NIR response increased, the overall efficiency of the cell decreased due to higher charge recombination at the interfaces. In a more successful study in 2010, Xie et al [129] constructed DSSCs with Yb^{3+} - Er^{3+} co-doped into the TiO2 thin film layer. This converted 980nm unabsorbed light into visible wavelengths 510-700nm which could be used by the cell. Under a solar simulator the cell achieved an efficiency of 7.28% compared to 6.41% for the un-doped DSSC, representing a substantial relative efficiency increase of 13.6%. In synthesis optimization studies it was found the DSSC with a TiO_2: RE ratio of 1:3 had the greatest efficiency. A beneficial secondary effect of directly inserting rare earths into the oxide is that it acts a p-type dopant, raising the Fermi level of the electrons in the oxide and the redox potential in the electrolyte, therefore increasing the photo voltage of the DSSC. In 2013 Ramasamy and Kim [130] took a different approach in applying UC to DSSCs. They produced a novel rear structure with silver reflectors and Fe^{3+} doped β-$NaGdF_4$: Yb^{3+} - Er^{3+} UC nanoparticles (UCNPs). Iron had been found to increase the UC emission by a factor of 30 and the silver particles further enhanced the process by 2 possible effects – increased scattering or surface-coupled plasmon emission. The latter is an area of great interest to improving UC in solar cells since overlap between a plasmonic resonance frequency and UC emission spectra can lead to faster radiative decay rates in the UCNPs, increasing the intensity of the luminescence. A 2017 study by Han et al [131] used hollow Er^{3+} - Yb^{3+} CeO_2 spheres as UCNPs and reported a 27% relative increase in PCE for a DSSC.

3.6.2 Organic Solar Cells

Organic Solar Cells (OSCs) are polymer based photocurrent generating structures and like DSSCs they are lightweight and cheap to produce. Common compounds used in OSC fabrication include conjugated polymers such as polyphenylenevinylene (PPV) derivatives or poly [3-hexylthiophene] (P3HT) with a fullerene derivative (PCBM) [132]. As with all solar cells, OSCs suffer IR losses from a limited absorption range which stops at 800nm. Therefore UC has potential to improve their efficiency.

In 2012 studies by Wang et al [133] added a composite layer of $Yb3^{+}$-Er^{3+} co-doped MoO_3 beneath the photoactive P3HT/PCBM region of the OSC. A modest increase in short-circuit current of < 1% was observed under 1 sun. If greater improvements were to be made there would need to be developments in UCQY, employment of light trapping/management and thicker up converting films. Over the same period, Damitha Adikaari et al [134] instead used Ho^{3+}-Yb^{3+} co-doped Y_2BaZnO_5 on organic PV devices to obtain an EQE of 0.0052% under illumination by a 986 nm laser. Despite this small value they showed a wider excitation spectrum and additional modifications such as transparent electrodes could lead to values more like those achieved in amorphous silicon cells and an overall conversion efficiency rise of 0.45%. In 2014 Chen et al [135] employed $Yb3^{+}$-Er^{3+} doped β-$NaYF_4$ UC particles in a polymethylmethacrylate (PMMA) matrix and a silver reflector to an OSC. They observed a 22.2% enhancement in the short-circuit current density; however, a large portion of this was due to visible light being reflected. Despite demonstrating technical feasibility, they attribute only 1.6% of the photocurrent enhancement to the UC process and poor performance under

ambient solar conditions mean it is unlikely to be practically applied unless further improvements are made. Zhao, Ji and Guo reviewed a range of organo-transition metal complexes that could be used as sensitizing and accepting molecules in such a system [136]. Schulze et al [137] tested this through theoretical models and experimentally on three solar cells: two heterojunction OSCs (P3HT: ICBA and PCDTBT: PC71BM) and one a-Si. They showed proof-of-principle but again the measured short-circuit current enhancements were negligible, only 0.2%, 2-3 orders of magnitude below a device relevant value. However, TTA still may be promising over conventional rare earth ETU because of higher quantum efficiency. Furthermore the models showed sensitizer concentration was the key parameter to be optimized but was difficult to achieve the desired levels in the organic solvent. They suggested incorporating the molecules into solid state compounds such as nano-particles or polymer films as a way to get round this.

3.6.3 Quantum Dot Solar Cells

QD solar cells (QDSCs) are an emerging technology that have attracted considerable interest as yet another low cost alternative to traditional silicon cells [138]. Despite tuneable absorption spectra, there will always be wavelengths that a manufactured QD cannot absorb beyond, so one would expect there is again potential for their use in conjunction with UC devices. Until recently there were few examples of UC being applied to QDSCs. However, in a recent study by Wang et al [139] in 2014, a Tm^{3+} - Yb^{3+} - Er^{3+} tri-doped $NaYF_4$ phosphor was synthesised and annealed, then introduced to the photoanodes of a CdS/CdSe QDSC. A maximum PCE of 4.37% was achieved, marking a 20% increase and 17.6% enhancement of the photocurrent. The annealing pre-treatment is a contributing factor to this excellent result as it eliminates defects which reduce charge recombination in the cell. Furthermore in 2017, Ramachari et al [140] have explored the effects of incorporating Yb^{3+} - Er^{3+} co-doped ZrO_2 into a QDSC, leading to a 55% relative increase in the PCE.

3.6.4 Perovskite Solar Cells

An emerging PV technology known as perovskite solar cells (PSCs) are hybrid organic-inorganic devices based on the crystal structure called perovskite [141]. Their low cost and easy fabrication makes them a promising candidate in PV systems, and they demonstrate reduced charge carrier losses and significantly improved stability as compared to DSSCs [142]. Recent developments in their design has led to a rapid growth in power conversion efficiency; 3.8% in 2009 to 6.5% in 2011 with a 20.1% system being verified by National Renewable Energy Laboratory (NREL) by the end of 2015 [143]. These cells absorb between 300 and 800 nm so like other nanostructured and thin film technologies could benefit from a UC (and/or DC) layer in order to use a greater portion of the solar spectrum. This was envisaged by Wang [144] and in recent studies UC crystals or nanoparticles have been successfully integrated with PSCs to give modest efficiency increases. There have been different approaches in choosing where to put the UC materials. For example Chen et al [145] applied a visibly transparent $LiYF_4$: Yb^{3+}, Er^{3+} single crystal on top of a PSC to increase the PCE by 7.9% under 7-8 sun illumination, whereas He at al [146] and Roh et al [147] have added the UCNPs in situ by combining them with the mesoporous electrode, the latter

attaining a 13.7% PCE enhancement and latest results by Wang et al have shown a 20.8% improvement [148]. As with DSSCs there may be extra benefits to an internal addition of nanoparticles such as the aiding of quality perovskite crystal growth during the device fabrication.

Table 2 – Summary of UC investigations carried out on various types of solar cell.

4. Downconversion experiments

In addition to losses from sub-band gap photons it is estimated an even greater proportion of the solar spectral energy (recalling Fig. 1) lost from photons possessing too much energy. In silicon solar cells, a photon with energy greater than the band-gap will create an electron-hole pair but the once in the conduction band the charge carrier has excess energy which will mostly be lost as dissipated heat. Cells also have an optimal EQE that varies with wavelength (cf. Fig.6) so in theory getting as much of the spectrum as possible at that energy would be an excellent way to improve efficiency. Although contrary to UC, lower band gap cells or systems with a poor UV response stand to gain the most from an efficient DC layer.

4.1 Working principles of downconversion

Owing again to their diverse energy structure, rare earth materials have considerable potential for DC devices. Many of the responsible mechanisms for DC appear analogous to UC but in reverse. In their 2013 article Huang et al [149] describe five processes as typical. Firstly, a mechanism equivalent to GSA/ESA in reverse, a UV photon is absorbed in a single ion, promoting an electron from the ground state to a secondary excited state before decaying sequentially, emitting two NIR photons. There also exist three possible routes for DC via resonant energy transfer between two distinct ions as shown in the figure. Finally, a reverse co-operative energy transfer takes place when an ion absorbs a photon and transfers the energy to two additional ions promoting them to an excited state. These states then simultaneously decay emitting two low energy photons. Despite these similarities it has been shown unlike UC, DC tends to be a linear process independent of light intensity [150].

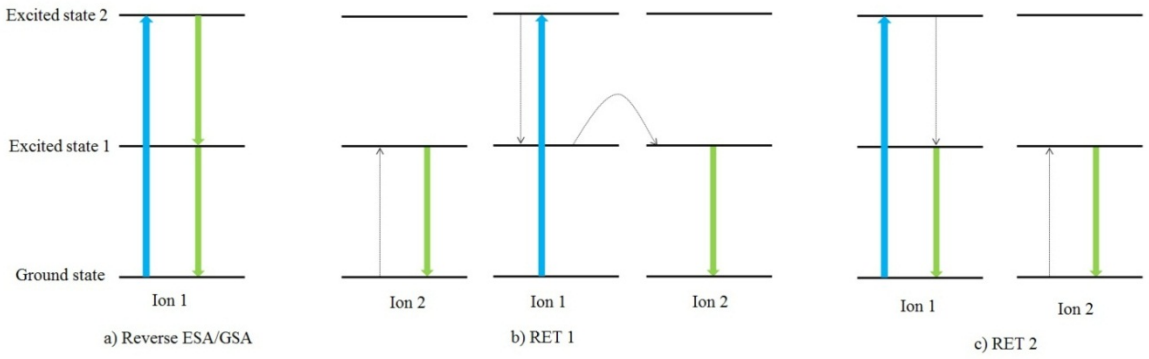

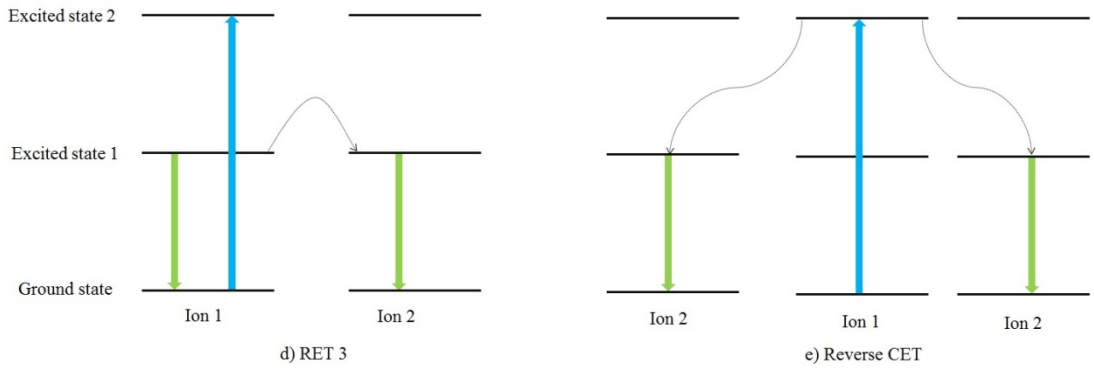

Fig. 11. Diagram of the main mechanisms for downconversion: a) ESA in reverse b) c) and d) resonant energy transfer between two ions and e) CET. Figure modified from [149].

4.2 Downconversion materials

The DC process has been observed in several lanthanide compounds and from observing the energy transfer efficiency in RE ions, theoretically attainable e-PLQYs greater than 150% [151] (in cases approaching 200% [152]) have been consistently reached (cf. Equation 1, the maximum possible quantum yield for a DC process will be 200%). Direct measurements of e-PLQY are rarer in the literature but a value of over 100% has been reported [153]. Despite this and Trupke's earlier promising analysis, in 2007 Strümpel et al [154] concluded DC to have little practical promise in terrestrial PV due to the high excitation energies required falling within UV light which is mostly blocked by the atmosphere. A further problem arises from having to place the DC material on top of the solar cell which leads to parasitic absorption and scattering losses, meaning an e-PLQY of 115% would be required just to break even [155]. Nevertheless, research in this field continued with Huang et al cataloguing many studies from their 2013 review of both single ion and paired ion lattices [156]. The addition of other species can sensitize the DC process by increasing the absorption cross section. These have often taken the form of divalent rare earth ions such as Eu^{2+} and Yb^{2+} or transition metal ions such as Mn^{2+}. Tai et al [157] demonstrated Eu^{2+} acted as an efficient energy sensitizer for Yb^{3+} in a $SrAl_2O_4$ lattice, reaching a quantum efficiency of 147.36% under illumination by a 450 W xenon lamp. The broadband 250-450 nm light was shifted to 980 nm where it could be effectively utilised by a silicon solar cell. Most studies have implied use for c-Si but from Fig. 6 it's clear other technologies could benefit too, such as Ge cells with their very low band gap of 0.67eV (1850 nm). As with UC, it is important to carefully select the dopant concentration and layer thickness to minimise self-absorption losses. Boccolini et al have presented an optical model to determine the optimal thickness of a DC layer which was validated by experimental analysis of a Ce^{3+} - Yb^{3+} co-doped borate glass [158]. Li et al [159] have also demonstrated broadband DC in Yb^{3+} doped $Na_2YMg_2(VO_4)_3$ which under UV illumination 240-400nm showed intense NIR emission at 974nm, ideal for silicon cells. By analysing decay curves a mechanism based on combined energy

transfer was proposed. For a recent review focussing exclusively on the available DC materials and their application to PV the reader is referred to [160].

4.3 Downconversion applications for silicon PV

Until recently there had been few physical DC-PV systems fabricated and their efficiency enhancements recorded. However there have been an increasing number of studies since 2015. That year, Dumont et al [161] prepared Tb^{3+} - Yb^{3+} co-doped Silicon-Nitride matrix DC layers via magnetron co-sputtering. By using novel optimization techniques and material characterization, its yield was improved from prior studies and was deemed to be suitable for application to a silicon solar cell, due to efficient of emission of 980 nm light following 325 nm illumination. It also had anti-reflective coating properties, a further reason for this being an excellent candidate for being placed atop an actual silicon cell. Gonzales-Perez et al [162] have further considered these design properties with their Eu^{3+} complex embedded in PMMA which was applied to a reference silicon cell by spin coating or tape casting. The EQE of the cell increased by 5.8% at 280 nm illumination due to a strong UV excitation band from 250-360 nm with emission at 665 nm. The film also showed excellent thermal stability meaning it could easily be applied in the module assembly of silicon cells and be used in CPV. Additionally, Florêncio et al [163] reported a 7% enhancement in the efficiency of a commercial silicon cell when Tb^{3+} - Yb^{3+} co-doped tellurite glass was placed on top as compared to un-doped glass.

4.4 Downconversion applications for emerging PV

DC particles have also been applied to emerging PV cells. In a novel investigation Yao et al [164] enhanced the conversion efficiency in a DSSC to 4.8% (an improvement of 245% from pure TiO_2) using Eu^{3+}-Dy^{3+} co-doped ZnO applied to the TiO_2 photoanodes alongside graphene loading to reduce recombination and interfacial resistance. Similarly in 2016, Hou's group have reported a Eu^{3+} doped $ZnGa_2O_4$ nanophosphor in the porous TiO_2 of a PSC [165]. This led to an enhanced short-circuit photocurrent by a maximum of 4.08 mA/cm^2 and relative power conversion efficiency increase of 34.4% due to improved light harvesting.

Table 3 – Summary of DC investigations carried out on various types of solar cell.

5. Luminescent downshifting experiments

5.1 Luminescent downshifting materials

Rare earth doped phosphors [166], organic dyes [167] and QDs [168] have all been suggested to be utilised for achieving LDS structures for PV cells. The responsible mechanisms will vary by material and do not appear to be as widely discussed in the literature as per the rare earth ion energy level diagrams described for UC/DC.

However, Huang et al [169] outline five key characteristics for LDS materials:

1. Broadband absorption, particularly in regions of poor spectral response for the relevant solar cell
2. High absorption coefficient and quantum efficiency
3. High transmittance and narrowband emission in region of high device response
4. Large Stokes shift to minimise self-absorption losses
5. Long term stability

Rothemund et al presented a simple, analytical optical model to calculate the potential EQE gains for various solar cell technologies following the addition of an LDS layer. This could be useful in future studies for evaluating experimental data, optimizing LDS layers and screening potential LDS materials [170]. In another investigation Lipovšek et al [171] used 3-D ray tracing and Mie scattering theory, to produce an experimentally verified model which predicted OSCs could gain 6% short-circuit current from an LDS layer. The model accounted for several parameters such as layer thickness, phosphor size distribution and volume concentration. Furthermore, Lesyuk et al [172] have explored cadmium-free QDs as a non-toxic alternative to the often used CdSe/ZnS QD.

5.2 Luminescent downshifting applications for silicon PV

Hung and Chen [173] prepared a Eu^{3+} doped gadolinium oxysulfide layer for a mc-Si solar cell. Under ambient solar illumination conditions an enhancement in J_{SC} of 6.47 mA/cm^2 and power conversion efficiency of 2.67% was observed. This material was simple and low cost to produce and also acted as an anti-reflective coating, reducing losses from Fresnel reflection. Similarly, Ho et al [174] used two Eu^{2+} doped phosphor species mixed with SiO_2 and spin coated the solution on a single silicon solar cell. The cell's J_{SC} increased 19.85% and relative PCE by 15.97% due to a combination of broadband (512-610 nm) emission and forward scattering. Tm^{3+} doped fluoride glasses have also been investigated for their LDS properties and combined with a c-Si cell. Maalej et al [175] reported a modest 1.4% relative PCE enhancement at a 1% Tm^{3+} doping concentration when compared to un-doped glass. They concluded a greater absorption and collection of converted photons was needed to scale up these glasses for commercial application.

5.3 Luminescent downshifting applications for thin film PV

2nd generation PV technologies such as CdTe or CIGS cells would stand to benefit a lot from LDS due to their very poor short wavelength response (cf. Fig. 6). These are thin film semiconductors intended to attain lower pay back times and less environmental impact than 1st generation c-Si modules [176]. A typical cell consists of a layer of CdTe or CIGS in contact with CdS to form a p-n junction [177]. Uekert et al [178] recently prepared nanostructured organosilicon luminophores embedded in ethyl vinyl acetate (EVA) or polyvinyl butyral (PVB) to act as an LDS layer for a CIGS cell. The device showed a remarkable improvement in EQE in the UV region from 1% to 55% at 360nm and a relative PCE increase of up to 4.3%. Alternatively, Ross et al [179] applied organic dye-doped EVA and fluorinated ethylene propylene (FEP) cover sheets to two CdTe modules which improved the short-circuit current by 9.7% and 5.3% respectively. Meanwhile Hodgson et al [180] have explored varying concentrations of semiconductor QDs encapsulated in a PMMA film over a thin-film CdS/CdTe cell. They found an overall efficiency gain of 1.7% for a QD concentration 48 μg/mm^3. In most recent studies by Song et al [181] Mn^{2+}-Eu^{3+} co-doped phosphate glasses were applied to CdS/CdTe cells for a relative increase in power conversion efficiency of 7.14%. It was also noted how the thickness of the LDS layer is a key parameter in determining overall efficiency gains; a thicker layer leads to more increased photocurrent at short wavelengths but will also lead to more absorption of the desired wavelengths and hence losses. Concentrating LDS has also been investigated as material that simultaneously shifts wavelength and increases intensity would be most beneficial atop a solar cell. In one such study Parel et al [182] tested different LDS structures on a CdTe/CdS solar cell. The measured current output increased 10% by the addition of a concentrating LDS, compared to 5% without the light concentration. Furthermore, the addition of other species into the layer improved the energy transfer and spectral absorption, resulting in an ultimate 20% enhancement in the short-circuit current.

Table 4 – Summary of LDS investigations carried out on various types of solar cell.

6. Enhancing spectral modification via nanostructures

As advances in nanotechnology have progressed, it has been possible to engineer nanostructures to the benefit of spectral conversion (particularly the UC process). One of the key drawbacks of increasing solar cell efficiency via UC is the rare earth doped material's limited absorption spectrum. When we compare their optimum absorption wavelengths to the AM1.5G spectrum (cf. Fig 19), we see there are large parts of the sub-band gap region that do not undergo UC; the 1050-1350 nm and 1580-1800 nm range is not utilised by either Yb^{3+}-

Er^{3+} or Er^{3+} ions where they are attempting to improve the efficiency wide band gap or c-Si PV respectively.

6.1 Quantum dots

QDs have been explored as a potential way to overcome this problem and enhance emission from rare earth ion based UC layers [183]. In 2010 Pan et al [184] combined an Yb^{3+}-Er^{3+} doped oxide UC layer with PbS QDs. The addition of the QDs effectively widened the absorption spectrum by absorbing photons that would otherwise be transmitted and re-emitting at wavelengths that could be utilized by the UC ions. When applied to a bifacial silicon solar cell, a 60% increase in photocurrent was observed under IR illumination for the PbS-UC layer than the UC layer alone.

6.2 Photonic crystals

Further still improvements can be made by making use of another nanostructure, photonic crystals. Photonic crystals are optical nanostructures that influence a photon's behaviour in a solid [185]. Therefore they can be very useful for UC-PV, where direction and wavelength of light undergoing interaction is critical for the process' efficiency. In 2015 Marques-Hueso et al [186] coupled PbSe QDs with InP graphite lattice photonic crystals for a remarkable improvement in UC properties. The photonic crystal acted as a wavelength modifier by further shifting the QD emissions (reducing re-absorption) and concentrating the spectrum in the region where the rare earth absorption is strongest. This led to a 158% increase in the amount of QD emission matching the upconverter absorption. Furthermore, the vertical emission grew by a factor of 7.8 which would be beneficial for a spectral concentrator located beneath a bifacial cell as it significantly reduces scattering, meaning more photons reach the cell.

6.3 Core-shell nanostructures

The small physical size of the UC ions or nanoparticles is also problematic for the process' efficiency [187]. This results in a small cross section leads to low quantum yields even at absorbing wavelengths. One possible route is the addition of antenna ligands to the UC ions, in order to increase the absorption cross section. In one such study Zou et al [188] observed a 3300 enhancement in UC luminescence by using a cyanine dye (IR-806). Further developments in the use of dye ligands to enhance UC are discussed in a recent letter by Huang [189]. The creation of UCNPs in a core-shell design has also been proposed to overcome this [190]. These UCNPs would typically consist of a core of rare earth ions surrounded by a shell of phosphor and insulator (for example SiO_2) to achieve electrical isolation of the up converting metal and reduce recombination. Furthermore, it is possible to construct UCNPs with a multi-shell structure with each layer containing distinct RE ions,

allowing for greater broadband excitation. Investigations by Shao et al [191] have successfully shown these designs can absorb a wider part of the spectrum, 270 nm in their case. The use of inert layers helped the process by ensuring each ion acted in isolation and to minimise cross relaxation losses.

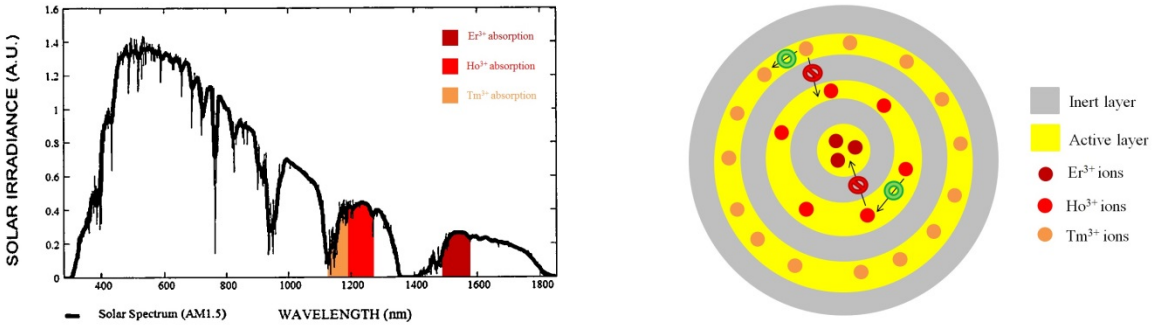

Fig. 12. 2-D cross-section schematic of core-shell nanostructure with distinct ions in each active region. The ions absorb at distinct wavelengths and are separated by an inert layer which prevents the different elements from interacting with one another. The expanded absorption range from 1120-1260 nm is shown on the AM 1.5 solar spectrum. Figure modified from [191].

6.4 Plasmonic nanostructures

An additional nanoscale phenomenon that can benefit UC is plasmonic resonance [192] Plasmons are quasiparticles that are the quanta of vibrations in the electron density in metals. Surface plasmon resonance can occur at the boundary of two materials when the frequency of incoming radiation matches that of the oscillation of the electrons [193], leading to increased photon intensity being emitted from the surface. Such an effect could be useful for UC where the converted light has a low intensity. In practice these are often combined with core-shell design UCNPs. Atre et al [194] constructed an upconverter doped dielectric core encased in a crescent-shaped Ag shell. They calculated a 100 fold increase in the above band-gap power emission towards the cell. They concluded that these nanostructures would eventually enable low-cost single junction solar cells that exceed the Shockley Queisser limit. This concept has been successfully employed to a DSSC by Liu et al [195] who prepared Au-decorated core-shell β-$NaYF_4$:Er^{3+}/Yb^{3+}@SiO_2 UCNPs. The UC was able to induce localised surface plasmon resonance which increased the absorption of the dye sensitizer and hence the photocurrent response. Luoshan's group [196] also employed a similar method but their UCNPs had an additional @TiO_2 shell layer to provide a transport channel for generated electrons, enhance dye loading and isolate the Au from the electrolyte. These effects can also complement other nanostructures for even greater effect. Le and John [197] proposed synergistic plasmonic and photonic crystal trapping of light to enhance the UC process in thin film solar technologies. They modelled a slanted conical photonic crystal structure atop core-shell rings and a UC layer. It was found the IR light intensity in the UC region could reach

1400× the ambient solar spectrum, allowing for a much more efficient UC process. An additional beneficial effect for practical considerations was the improved light trapping and absorption spectrum for light at incident angles of up to 60º. Furthermore, Ahmed et al have for the first time demonstrated plasmonic LDS using QDs and Ag-UCNPs, resulting in a 60% increase in emission intensity and 22% rise in J_{SC} for both silicon and DSSCs over the 300-500nm illumination range [198].

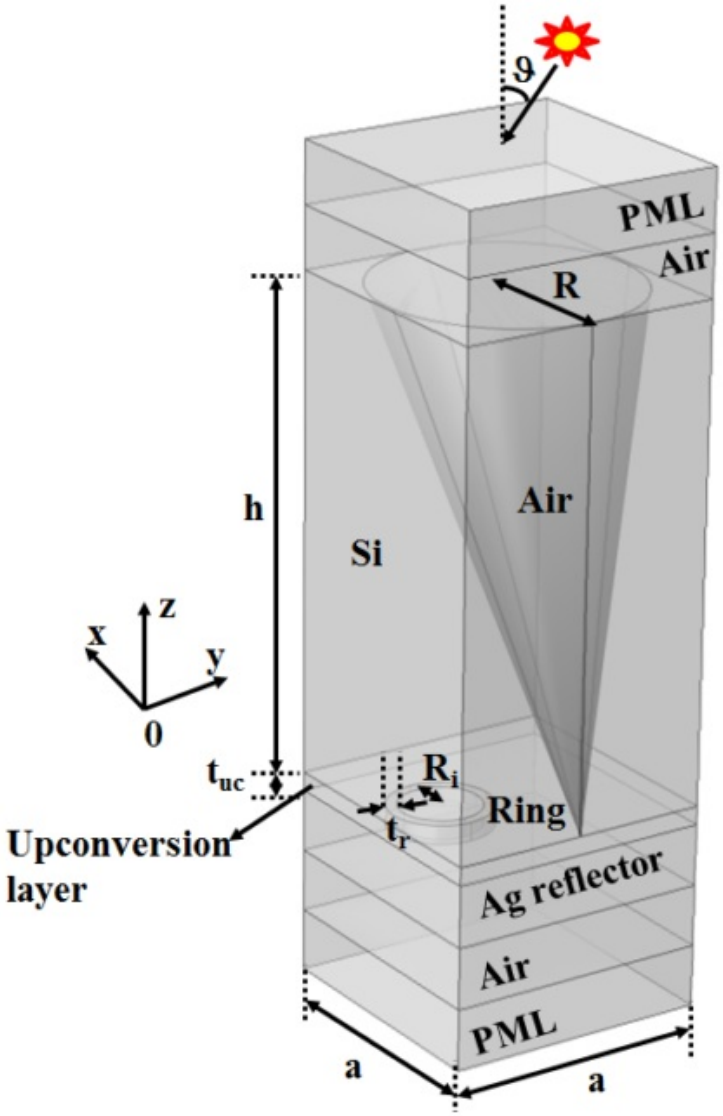

Fig. 13. The unit cell of the synergistic plasmonic and photon crystal structure with perfectly matched layers, denoted PML. Figure taken from [197].

7. Discussion: challenges and opportunities

As presented over the last decade there have been significant advances in UC; from a largely conceptual field to the construction of efficiency enhanced physical systems. However despite this progress the overall efficiency increases are modest at best and are yet to surpass the Shockley-Queisser limit as predicted or be suitable for mass commercial deployment. We must therefore ask what further progress must be made, if we are to defeat these challenges

and utilise spectral conversion for solar cells in the world energy market as an alternative to fossil fuels?

The development of dedicated solar cells for UC-PV is a critical area of research to take this field forward. Rüdiger et al [199] present ways to practically implement these designs by identifying three criteria for a bifacial solar cell being used in an up converting system to fulfil: a very high transmittance to photons of wavelength < 1200nm to illuminate the UC layer, a high EQE when illuminated by upconverted photons from the rear and a high efficiency itself to optimize the system. From UC data as of 2014 they found this could reasonably attain a 3% relative enhancement in overall efficiency and then fabricated a bifacial n-type silicon solar cell which achieved an EQE of 1.69% under 1508nm illumination (5 times higher NEQE than non-optimized cells). They concluded both sides being textured rather than planar improved performance and the double-layer ARC helped reduce optical losses. Further aspects for consideration are the external electronic circuit and ensuring minimal interference with the UC system and the ultimate design for physical deployment in panels of these structures. For example, how would they have the long term stability of on the market modules? There needs to follow a comprehensive classification of materials, including the ones presented in this review, for their effectiveness in increasing over all solar cell efficiency. It can then eventually be decided which materials are prime for adaptation in real systems; Er^{3+} / Er^{3+} - Yb^{3+} doped $NaYF_4$ or its competitors? The recent review on advances in $NaYF_4$ luminescence by Kumar et al [200] or a comparative analysis between fluorides by Favilla et al [201] are examples of this. A range of experimental synthesis techniques have been reported for the preparation of spectral modification materials in the studies referred to throughout this paper. Although discussing general optimization parameters such as doping concentration, polymer weight ratio and choice of materials, it is worth comparing the fabrication procedures as these will impact viability of research (since the reader may wish to know what can be constructed in their lab) and potentially commercialization. The costs and environmental impact of each method should be a matter for debate. Verification procedures such as x-ray diffraction, scanning electron microscopy and differential scanning calorimetry are widely used throughout the literature. These techniques should be utilized along with further modelling studies to maintain a decent theoretical understanding of the underlying mechanisms.

Concentrator-UC systems, with components operating at distinct spectral intensities (cf. Fig. 18) must be greater looked into and for a range of materials. Two-photon lithography allowing for the microscale construction of optics could be an exciting area to develop UC concentrators for thin film solar technologies [202]. The new fields of UC via thermal radiation and QDs can be contrasted for efficiency gains in these conditions as well, especially the latter since practical applications of that approach are lacking due to high concentrations required. The use of novel new materials like graphene may also aid the QD approach to UC being tested experimentally. Zhang et al [203] have reviewed the remarkable properties of graphene QDs for a range of applications including solar PV and in 2013 Lee et al [204] fabricated them and tested their effects on DSSCs.

TTA-UC, again lacking applications to cells in the literature may prove to be an attractive route to increasing solar cell efficiency in the near future. Not only does its low required light intensities offer simpler deployment (perhaps eventually to areas of low-moderate DNI) but from a financial perspective its fundamental materials are not too expensive either. Schulze advocated zinc poryphins to sensitise TTA-UC systems, which still give high efficiencies but at a fraction of the cost of heavier metals (since zinc is only approximately $2/kg) [205]. However as with many emerging photochemical technologies further research is needed into oxygen defence and encapsulation in order to prevent photo-degradation. To support this outlook, recently Wu's group have prepared solid state TTA-UC materials that utilize thermally activated delayed fluorescence molecules and noted the lack of heavy metals such as Pt or Pd could lower costs if the technology becomes widespread [206]. To further maximise potential enhancement to PV performance, multi-mode or broadband UC devices should be constructed and their benefits to solar cell efficiency compared with (or even combined with) materials that increase a given ions absorption spectrum. These steps of research could help to take UC experiments beyond their meagre increases in overall cell efficiency. Multimodal phosphors either in separate layers as proposed by Lahoz or in Shao's group's UCNPs designed in 6.3 should be tested for efficiency improvements and compared with what can be achieved through spectral conversion aided by the use of QDs. Since for spectral conversion to be a realistically viable approach it will have to capture as much of the spectrum as possible.

This author would propose further investigations drawing advice from this review, into a range of solar cells including the very latest emerging technologies which have only recently been investigated for UC/DC applications. DC/LDS should be applied to more solar cells, especially those made from c-Si and CdTe as despite recent progress testing for overall efficiency measurements is still less frequently reported than UC. Also it was felt DC/LDS lacked the comprehensive optimization studies and standard lattices prevalent in the UC literature, so this should be an area of research interest in the near future. Simultaneous up and DC is a concept that should also be explored, to *both* harness sub band-gap photons *and* reduce losses from photons with excess energy. This could in theory highly enhance photon energy or at least surpass the Shockley-Queisser limit while allowing for imperfections in each conversion layer. There is very little experimental research into this, partly because of a number of physical dilemmas it raises. The addition of a DC or LDS layer raises the issue of photons of wavelengths desirable to the solar cell below being absorbed into the conversion layer and it crucially must have very high transmission to photons of UC energies. One proof-of-principle experiment for this concept was carried out by Yao et al [207] in which rare earth doped zinc oxide up and DC layers were introduced into a DSSC. Er^{3+} and Yb^{3+} were used for the UC layer, Eu^{3+} and Tb^{3+} for the DC. The DC layer also acted to reduce charge recombination. A 70% enhancement in efficiency was observed in comparison to the standard DSSCs, one of the largest relative increases cited in this review. In another recent novel study, Lee et al [208] designed and fabricated a metal nanodisk-insulator-metal structure which simultaneously enhances UC and LDS luminescence via plasmonic resonance. It was created by a nanotransfer printing method which can easily replicate this structure over a large area and achieved outstanding enhancements of UC and LDS intensity

by factors of 174 and 29 respectively. These improved modifications from both NIR and UV to visible could have remarkable potential in capturing even more of the solar spectrum for a wide band-gap cell. Materials that can operate as up or down converters may reduce costs in making these types of systems. Same material, multi-modal UC and DC emission has been observed in compounds such as Er^{3+} doped K_2YbF_5 [209], Tb^{3+} - Yb^{3+} co-doped lithium borate glass [210] and Tb^{3+} - Yb^{3+} co-doped $GdPO_4$ [211] which could all be attractive for PV applications. Additionally, efficient DC has been reported in rare earth doped α-$NaYF_4$ [212] which contains the same elements and could be synthesised alongside the popular UC phosphor β-$NaYF_4$.

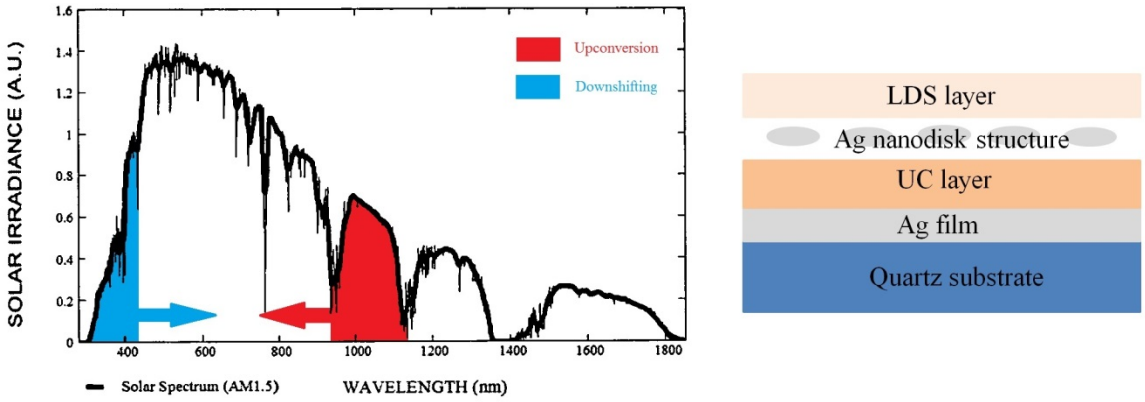

Fig. 14. Graphical representation of the promising simultaneous spectral conversion (UC and LDS) and the schematic of the layers fabricated. Figure modified from [208].

Finally, a quantitative financial comparison must be made between spectral modification and competing solutions to surpassing the Shockley-Queisser limit, building on the cost analysis work which came from the EPHOCELL project [213]. Multijunction cells use many expensive materials and are difficult to fabricate, resulting in a high cost per watt even with the use of concentrators, so a cost-effective efficient spectral modification layer on a single junction cell could still be a sensible solution over multi-junction CPV. To demonstrate this point mathematically we derive the condition for an efficiency enhancing modification to lower the cost per peak watt. First, consider a single junction cell of arbitrary area with a cost C_{cell}, maximum power output P_{max} and cost per peak watt C_{cell} / P_{max}. Then if a modification layer with cost $C_{modification}$ is added to give a relative increase in efficiency ΔPCE, the new cost per peak watt will be:

$$New\ cost\ per\ watt\ peak = \frac{C_{cell} + C_{modification}}{(1 + \Delta PCE)P_{max}} \qquad \text{(Equation 5)}$$

This can be used to directly compare costs with other approaches. Furthermore, comparing the above equation with the cost per watt peak of the original cell and dividing by C_{cell} / P_{max} yields the condition for the modification to lower the cost per watt peak:

$$\frac{1 + \frac{C_{modification}}{C_{cell}}}{1 + \Delta PCE} < 1 \quad \text{(Equation 6)}$$

By using equation 12, approximate rare earth prices (assuming they dominate compared to the lattice material), solar cell costs from Table 1 and the results from state of the art studies presented in this review, an important estimation can be determined: the maximum mass of rare earth than can be added per W of cell whilst still reducing the cost per W. Similar methods and cost analysis by Ross which calculated the cost per W of power generated [214] are a useful exercise and should be considered in future spectral modification studies. Le Donne et al carried out a simple cost analysis [215] from their LDS Eu^{3+} complex on silicon experiment and estimated the price per watt peak could fall by €0.06 if a 0.65% enhancement in the J_{SC} could be obtained and the EPHOCELL project predicted similarly promising economics. Given the current data for efficiency gains this may be the only likely way for UC or DC to emerge into the market; small efficiency gains at a small cost per unit area.

Table 5 – Approximations for the maximum mass of rare earth ions that can be added per W of solar cell to still reduce the cost per W.

If these practical efficiency gains are to be realized then the nanostructures discussed should be applied to more physical set ups, in order to see if their reported effects can translate to greater PCE enhancements. Advances in simulations based on rate equations will allow theoretical models to predict and aid their implementation in physical systems. However, their development may prove expensive if they are to be implemented on a larger scale. Furthermore, rare earth metals necessary for up converting ions are also costly components [216], so we must consider their financial contribution to the construction of UC solar panels. For DC and LDS, whether the ions are doped into encapsulate glasses or applied directly via a thin film will influence cost. LDS glasses could be coloured to an aesthetically pleasing look, increasing their potential for building integrated PV. These factors should be investigated and a matter for debate, to justify if the relative efficiency gains are worth the added costs. Notwithstanding this competition, it may be possible to combine spectral conversion and tandem solar cell technologies. It has been proposed III-V silicon tandem cells may benefit from UC since the silicon component produces a lower current so would benefit more for a given UC performance [217]. It also may make sense to have a UC layer for the lowest band-gap material, since despite the use of multi-junctions widening the absorption spectrum they do not cover the whole solar spectrum. Although perhaps it is a futile exercise, as there is minimal energy to be gained from up converting photons with less energy than the narrowest solar cell band-gaps. Another solution to attain theoretical efficiencies above the Shockley-Queisser limit is multiple excitation generation (MEG); a

phenomena where an absorbed photon can excite more than one electron to the conduction band in a semiconductor. Investigations have led to peak EQE's of over 100% reported in a QDSC [218] and Shpaisman et al [219] concluded MEG and UC could be combined to give a PCE of 38% for a single junction cell, although at a very optimistic efficiency for processes (25% for UC and 70% for MEG).

8. Conclusion

We have reviewed spectral modification as a means to achieve greater solar cell efficiencies which is an important research area in the context of environmental issues and current engineering limitations. After briefly overviewing the theoretical basis for UC, DC and LDS, a number of studies have been presented that successfully attempt to apply these processes to harnessing greater energy from the solar spectrum. From the investigations using rare earth doped compounds, it seems the cells most likely to benefit from UC are wide band gap technologies such as amorphous silicon and DSSCs. On the contrary DC and LDS stand to improve cells with a poor UV response such as c-Si, CdTe and CIGS. However, all cells have an optimal wavelength for conversion efficiency, so as a handful of studies have tried, we may see more UC working together with DC or LDS on the same cell to efficiently shift as much of the incident spectrum towards this value as possible. The now commonly used c-Si cell appears to benefit from both upward and downward spectral modification, so this may be a focus of research although this depends on if emerging solar technologies improve towards commercial deployment in the coming years. Unfortunately, limitations arising from poor absorption and hence spectral conversion efficiency have prevented the exceptional gain in solar cell efficiency that is theoretically possible. However, nanoengineered phenomena such as plasmonic resonance and photonic crystals, in addition to macroscopic augmentations through concentrating optics have the potential to mitigate these drawbacks. Furthermore, novel new approaches such to UC via TTA, QDs or thermal radiation may aid in overcoming these problems. In conclusion spectral modification may not be the holy grail of solar cell design it first appears and in terms of performance is severely lagging behind concentrating multijunction PV. However, if research continues (including proposals in Section 7) while costs are kept low, investigations carried out may yield exciting prospects for expansion of solar PV.

Acknowledgements

Funding for study was provided by the Engineering and Physical Sciences Research Council (EPSRC) and is gratefully acknowledged.

References

[1] Shockley W, Queisser HJ. Detailed Balance Limit of Efficiency of p-n Junction Solar Cells. J Appl Phys 1960;32:510-9.

[2] National Renewable Energy Laboratory. Best research-cell efficiencies, https://phys.org/news/2016-02-solar-cell-efficiency-nrel.html; 2016 [accessed February 24 2017].

[3] Wiesenfarth M, Phillips SP, Bett AW, Horowtiz K, Kurtz S. Current status of concentrator photovoltaic (CPV) technology. Freiburg (Germany): Fraunhofer Institute for Solar Energy Systems, Golden, CO (USA): National Renewable Energy Laboratory; 2017 Apr. Report No.: TP-6A20-63916. Contract No.: DE-AC36-08-GO28308. Sponsored by the US Department of Energy.

[4] Patel K. Solar Panels Cost, http://solarenergyforus.com/solar-panels-cost/; 2016 [accessed Feb 24 2017].

[5] Semonin O, Luther JM, Beard MC. Multiple exciton generation in a quantum dot solar cell. SPIE Newsroom. 2012 Mar. doi: 10.1117/2.1201203.004146.

[6] Müller J, Rech B, Springer J, Vanecek M. TCO and Light Trapping in Silicon Thin Film Solar Cells. Sol Energy 2004;77:917-30.

[7] Singh P, Ravindra NM. Analysis of series and shunt resistance in silicon solar cells using single and double exponential models. Emerg Mater Res 2012;1:33-8.

[8] Cotal H, Fetzer C, Boisvert J, Kinsey G, King R, Herbert P et al. III-V multijunction solar cells for concentrating photovoltaics. Energy Environ Sci 2009;2:174-92.

[9] De Vos A. Detailed balance limit of the efficiency of tandem solar cells. J Phys D: Appl Phys 1980;13:839-46.

[10] Forbes D, Hubbard S. Solar-cell-efficiency enhancement using nanostructures. SPIE Newsroom. 2010 Jul. doi: 10.1117/2.1201007.003124.

[11] Araújo GL, Martí A. Absolute limiting efficiencies for photovoltaic energy conversion. Sol Energy Mater Sol Cells 1994;33:213-40.

[12] Xing Y, Han P, Wang S, Liang P, Lou S, Zhang Y et al. A review of concentrator silicon solar cells. Renew Sustain Energy Rev 2015;51:1697-1708.

[13] Kurtz S. Opportunities and Challenges for Development of a Mature Concentrating Photovoltaic Power Industry. Golden, CO (USA): National Renewable Energy Laboratory; 2012 Nov. Report No.: TP-520-43208. Contract No.: DE-AC36-08GO28308. Sponsored by the US Department of Energy.

[14] Baig H, Sellami N, Chemisana D, Rosell J, Mallick TK. Performance analysis of a dielectric based 3D building integrated concentrating photovoltaic system. Sol Energy 2014;103:525-40.

[15] Fraunhofer Institute for Solar Energy Systems ISE. New world record for solar cell efficiency at 46% – French-German cooperation confirms competitive advantage of European photovoltaic industry, https://www.ise.fraunhofer.de/en/press-media/press-releases/2014/new-world-record-for-solar-cell-efficiency-at-46-percent.html; 2014 [accessed February 24 2017].

[16] King RR. Fetzer CM, Law DC, Edmondson KM, Yoon H, Kinsey GS et al. Advanced III-V Multijunction Cells for Space. Proc 4th IEEE World Conference on Photovoltaic Energy Conversion; 2006 7-12 May; Waikoloa, HI, USA. p. 1757-62.

[17] Goldschmidt JC, Fischer S, Löper P, Krämer KW, Biner D, Hermle M et al. Experimental analysis of upconversion with both coherent monochromatic irradiation and broad spectrum illumination. Sol Energy Mater Sol Cells 2011;95:1960-3.

[18] Wolf M. Limitations and possibilities for improvement of photovoltaic solar energy converters. Proc IRE 1960;48:1246-63.

[19] Trupke T, Green M, Würfel P. Improving solar cell efficiencies by up-conversion of sub-band-gap light. J Appl Phys 2002;92:4117-8.

[20] Wegh RT, Donker H, Oskam KD, Meijerink A. Visible quantum cutting in $LiGdF_4:Eu^{3+}$ through downconversion. Sci 1999;283:663-6.

[21] Klampaftis E, Ross D, McIntosh KR, Richards BS. Enhancing the performance of solar cells via luminescent down-shifting of the incident spectrum: A review. Sol Energy Mater Sol Cells 2009;93:1182-94.

[22] Trupke T, Green M, Würfel P. Improving solar cell efficiencies by down-conversion of high-energy photons. J Appl Phys 2002;92:1668-74.

[23] Binetti S. Silicon based solar cells: Research progress and future perspectives. Proc 7th IEEE International Conference on Group IV Photonics; 2010 1-3 Sep; Beijing, China. p. 189-91.

[24] Huang X, Han S, Huang W, Liu X. Enhancing solar cell efficiency: the search for luminescent materials as spectral converters. Chem Soc Rev 2013;42:191.

[25] Yamada N, Anh LN, Kambayashi T. Escaping losses of diffuse light emitted by luminescent dyes doped in micro/nanostructured solar cell systems. Sol Energy Mater Sol Cells 2010;94:413-9.

[26] Zhang C, Sun L, Zhang Y, Yan C. Rare earth upconversion nanophosphors: synthesis, functionalization and application as biolabels and energy transfer donors. J Rare Earths 2010;28:807-19.

[27] Paskov PP, Holtz PO, Monemar B, Garcia JM, Schoenfeld WV, Petroff PM. Photoluminescence up-conversion in InAs/GaAs self-assembled quantum dots. Appl Phys Lett 2000;77:812-4.

[28] Lissau JS, Gardner JM, Morandeira A. Photon Upconversion on Dye-Sensitized Nanostructured ZrO2 Films. J Phys Chem C 2011;115:23226-32.

[29] Bloembergen N. Solid State Infrared Quantum Counters. Phys Rev Lett 1959;2,:84-5.

[30] Scheps R. Upconversion laser processes. Prog Quantum Electron 1996;20:271-358.

[31] Liu Q, Sun Y, Yang T, Feng W, Li C, Li F. Sub-10 nm Hexagonal Lanthanide-Doped $NaLuF_4$ Upconversion Nanocrystals for Sensitive Bioimaging in Vivo. J Am Chem Soc 2011;133:17122-5.

[32] Chen G, Ågren H, Ohulchanskyy TY, Prasad PN. Light upconverting core-shell nanostructures: nanophotonic control for emerging applications. Chem Soc Rev 2015;44:1680-713.

[33] van Sark WGJHM, Meijerink A, Schropp REI. Solar Spectrum Conversion for Photovoltaics Using Nanoparticles. In: Fthenakis V. Third Generation Photovoltaics, Rijeka, Croatia: InTech; 2012, p. 1-28.

[34] Shalav A, Richards BS, Green MA. Luminescent layers for enhanced silicon solar cell performance: up-conversion. Sol Energy Mater Sol Cells 2007;91:835.

[35] Dieke GH. Spectra and Energy Levels of Rare Earth Ions in Crystals, New York, NY, USA: Interscience; 1968.

[36] Shalav A, Richards BS, Green MA. Luminescent layers for enhanced silicon solar cell performance: up-conversion. Sol Energy Mater Sol Cells 2007;91:832-3.

[37] Chivian JS, Case WE, Eden DD. The photon avalanche: A new phenomenon in Pr3+-based infrared quantum counters. Appl Phys Lett 1979;35:124-5.

[38] Wang F, Deng R, Wang J, Wang Q, Han Y, Zhu H et al. Tuning upconversion through energy migration in core–shell nanoparticles. Nat Mater 2011;10:968-73.

[39] Strümpel C, McCann M, Beaucarne G, Arkhipov V, Slaoui A, Švrček V et al. Modifying the Solar Spectrum to Enhance Silicon Solar Cell Efficiency - An Overview of Available Materials Sol Energy Mater Sol Cells 2007;91:238–49.

[40] Yang H, Dai Z, Sun Z. Upconversion luminescence and kinetics in Er^{3+}:$YAlO_3$ under 652.2nm excitation. J Lumin 2007;124:207-12.

[41] Pollnau M, Gamelin DR, Lüthi SR, Güdel HU. Power dependence of upconversion luminescence in lanthanide and transition-metal-ion systems. Phys Rev B 2000;61:3337-46.

[42] Suvyer JF, Aebischer A, García-Revilla S, Gerner P, Güdel HU. Anomalous power dependence of sensitized upconversion luminescence. Phys Rev B 2005;71:125123.

[43] Anderson RB, Smith SJ, May PS, Berry MT. Revisiting the NIR-to-Visible Upconversion Mechanism in β‑$NaYF_4$:Yb^{3+}, Er^{3+}. J Phys Chem Lett 2014;5:36-42.

[44] Balda R, Hakmeh N, Barredo-Zuriarrain M, Medrignac-Conanec O, García-Revilla S, Arriandiaga MA et al. Influence of Upconversion Processes in the Optically-Induced Inhomogeneous Thermal Behavior of Erbium-Doped Lanthanum Oxysulfide Powders. Mater 2016;9:353.

[45] Baldo MA, Adachi C, Forrest SR. Transient analysis of organic electrophosphorescence. II. Transient analysis of triplet-triplet annihilation. Phys Rev B 2000;62:10967-77.

[46] Zhao J, Ji S, Guo H. Triplet–triplet annihilation based upconversion: from triplet sensitizers and triplet acceptors to upconversion quantum yields RSC Adv 2011;1:937-50.

[47] Baluschev S, Miteva T, Yakutkin V, Nelles G, Yasuda A, Wenger G. Up-conversion fluorescence: noncoherent excitation by sunlight. Phys Rev Lett 2006;97:7-9.

[48] Cheng YY, Nattestad A, Schulze TF, MacQueen RW, Fückel B, Lips K et al. Increased upconversion performance for thin film solar cells: a trimolecular composition. Chem Sci 2016;7:559-68.

[49] Dexter DL. A Theory of Sensitized Luminescence in Solids. J Chem Phys 1953;21:836–50.

[50] Singh-Rachford TN, Castellano FN. Photon upconversion based on sensitized triplet–triplet annihilation. Coord Chem Rev 2010;254:2560-73.

[51] Cheng YY, Fückel B, Khoury T, Clady RCGR, Tayebjee MJY, Ekins-Daukes NJ et al. Kinetic Analysis of Photochemical Upconversion by Triplet-Triplet Annihilation: Beyond Any Spin Statistical Limit. J Phys Chem Lett 2010;1:1795-99.

[52] Schulze TF, Schmidt TW. Photochemical upconversion: present status and prospects for its application to solar energy conversion. Energy Environ Sci 2015;8:103-25.

[53] Nozik AJ. Quantum dot solar cells. Phys E 2002;4:115-20.

[54] Deutsch Z, Neeman L, Oron D. Luminescence Upconversion in Colloidal Double Quantum Dots. Nat Nanotechnol 2013;8:649-53.

[55] Teitelboim A, Meir N, Kazes M, Oron D. Colloidal Double Quantum Dots. Acc Chem Res 2016;49:902-10.

[56] Shang Y, Hao S, Yang C, Chen G. Enhancing Solar Cell Efficiency Using Photon Upconversion Materials. Nanomater 2015;5:1782-809.

[57] Carlson TA, Krause MA. Experimental evidence for double electron emission in an Auger process. Phys Rev Lett 1965;14:390-2.

[58] Wang J, Tanner PA. Upconversion for White Light Generation by a Single Compound. J Am Chem Soc 2010;132:947-9.

[59] Keevers MJ, Green MA. Efficiency improvements of silicon solar cells by the Impurity photovoltaic effect. J Appl Phys 1994;75:4022-31.

[60] Gibart P, Auzel F, Guillaume JC, Zahraman K. Below band-gap IR response of substrate-free GaAs solar cells using two-photon up-conversion. Jpn J Appl Phys 1996;35:4401–2.

[61] Trupke T, Green M, Würfel P. Improving solar cell efficiencies by up-conversion of sub-band-gap light. J Appl Phys 2002;92:4117-8.

[62] Shalav A, Richards BS, Green MA. Luminescent layers for enhanced silicon solar cell performance: up-conversion. Sol Energy Mater Sol Cells 2007;91:838.

[63] Auzel F. Upconversion and anti-Stokes processes with f and d ions in solids. Chem Rev 2004;104:139-73.

[64] Wang F, Liu X. Recent advances in the chemistry of lanthanide-doped upconversion nanocrystals. Chem Soc Rev 2009;38:976-89.

[65] Johnson AR, Lee SJ, Klein J, Kanicki J. Absolute photoluminescence quantum efficiency measurement of light-emitting thin films. Rev Sci Instrum 2007;78:096101.

[66] Ahrens B, Löper P, Goldschmidt JC, Glunz S, Henke B, Miclea PT et al. Neodymium-doped fluorochlorozirconate glasses as an upconversion model system for high efficiency solar cells. Phys Status Solidi (A) Appl Mater Sci 2008;205:2827.

[67] Fischer S, Goldschmidt JC, Löper P, Bauer GH, Brüggeman R, Krämer K et al. Enhancement of silicon solar cell efficiency by upconversion: Optical and electrical characterization. J Appl Phys 2010;108:044912.

[68] Shalav A, Richards BS, Green MA. Luminescent layers for enhanced silicon solar cell performance: up-conversion. Sol Energy Mater Sol Cells 2007;91:833-834.

[69] Ermeneux FS, Goutaudier C, Moncorgé R, Sun Y, Cone RL. Zannoni E et al. Multiphonon relaxation in YVO_4 single crystals. Phys Rev B 2000;61:3915-21.

[70] Chung JW, Gerelkhuu Z, Oh JH, Li YI. Recent advances in luminescence properties of lanthanide-doped up-conversion nanocrystals and applications for bio-imaging, drug delivery, and optosensing. Appl Spectrosc Rev 2016;51:678-705.

[71] Vetrone F, Naccache R, Mahalingam V, Morgan CG, Capobianco JA. The Active-Core/Active-Shell Approach: A Strategy to Enhance the Upconversion Luminescence in Lanthanide-Doped Nanoparticles. Adv Funct Mater 2009;19:2924-29.

[72] Arnaoutakis GE, Marques-Hueso J, Ivaturi A, Krämer KW, Mallick TK, Richards BS. Enhancement of Upconversion for Photovoltaics with β- NaYF4:Er^{3+} and Concentrating Integrated Optics. Proc Optical Nanostructures and Advanced Materials for Photovoltaics 2013; 2013 3-7 Nov; Tuscon, AZ, USA. p. 9.

[73] Sun LD, Dong H, Zhang PZ, Yan CH. Upconversion of rare Earth nanomaterials. Annu Rev Phys Chem 2015;66:623

[74] Van Sark WGJHM, de Wild J, Rath JK, Meijerink A, Schropp REI. Upconversion in solar cells. Nanoscale Res Lett 2013;81:8.

[75] de Wild J, Duindam TF, Rath JK, Meijerink A, van Sark WGJHM, Schropp REI. Increased upconversion response in a-Si:H solar cells with broad bandlight. IEEE J Photovolt 2013;3:17.

[76] Huang X, Han S, Huang W, Liu X. Enhancing solar cell efficiency: the search for luminescent materials as spectral converters. Chem Soc Rev 2013;42:178.

[77] Ohwaki J, Wang Y. 1.3 μm to visible upconversion in Dy^{3+}- and Er^{3+}-codoped $BaCl_2$ phosphor. Appl Phys Lett 1994;65:129-31.

[78] Rodríguez-Rodríguez H, Imanieh MH, Lahoz F, Martín IR. Analysis of the upconversion process in Tm3+ doped glasses for enhancement of the photocurrent in silicon solar cells. Sol Energy Mater Sol Cells 2016;144:29–32.

[79] Yang W, Li X, Chi D, Zhang H, Liu X. Lanthanide-doped upconversion materials: emerging applications for photovoltaics and photocatalysis. Nanotechnol 2014;25:482001.

[80] Lahoz F, Pérez-Rodríguez C, Hernández SE, Martín IR, Lavín V, Rodríguez-Mendoza UR. Upconversion mechanisms in rare-earth doped glasses to improve the efficiency of silicon solar cells. Sol Energy Mater Sol Cells 2011;95:1671–7.

[81] Sun LD, Dong H, Zhang PZ, Yan CH. Upconversion of rare Earth nanomaterials. Annu Rev Phys Chem 2015;66:623.

[82] Krämer KW, Biner D, Frei G, Güdel HU, Hehlen MP, Lüthi SR. Hexagonal Sodium Yttrium Fluoride Based Green and Blue Emitting Upconversion Phosphors. Chem Mater 2004;16:1244-51.

[83] Suyver JF, Grimm J, Van Veen MK, Biner D, Krämer KW, Güdel HU. Upconversion spectroscopy and properties of $NaYF_4$ doped with Er^{3+}, Tm^{3+} and/or Yb^{3+}. J Lumin 2006;117:1–12.

[84] Patra A, Friend CS, Kapoor R, Prasad PN. Fluorescence Upconversion Properties of Er^{3+}-Doped TiO_2 and $BaTiO_3$ Nanocrystallites. Chem Mater 2003;15:3650-5.

[85] Richards BS, Shalav A. The role of polymers in the luminescence conversion of sunlight for enhanced solar cell performance. Synth Met 2005;154:61-4.

[86] Ivaturi A, MacDougall SK, Martín-Rodríguez R, Quintanilla M, Marques-Hueso J, Krämer KW et al. Optimizing infrared to near infrared upconversion quantum yield of β-NaYF4:Er^{3+} in fluoropolymer matrix for photovoltaic devices. J Appl Phys 2013;114:013505.

[87] Boccolini A, Marques-Hueso J, Richards B. Self-absorption in upconverter luminescent layers: impact on quantum yield measurements and on designing optimized photovoltaic devices. Opt Lett 2014;39:2904-7.

[88] Ivanova S, Pellé F. Strong 1.53 μm to NIR–Vis–UV upconversion in Er-doped fluoride glass for high-efficiency solar cells. J Opt Soc Am 2009;26:1930-8.

[89] Fischer S, Favilla E, Tonelli M, Goldschmidt JC. Record efficient upconverter solar cell devices with optimized bifacial silicon solar cells and monocrystalline BaY_2F_8:30% Er^{3+} upconverter. Sol Energy Mater Sol Cells 2015;136:127-134.

[90] Martín-Rodríguez R, Fischer S, Ivaturi A, Froehlich B, Krämer KW, Goldschmidt JC et al. Highly Efficient IR to NIR Upconversion in Gd2O2S: Er3+ for Photovoltaic Applications. Chem Mater 2013;25:1912-31.

[91] Goldschmidt JC, Fischer S, Löper P, Krämer KW, Biner D, Hermle M et al. Experimental analysis of upconversion with both coherent monochromatic irradiation and broad spectrum illumination. Sol Energy Mater Sol Cells 2011;95:1962.

[92] MacDougall SKW, Ivaturi A, Marques-Hueso J, Krämer KW, Richards BS. Enhanced up-conversion for photovoltaics via concentrating integrated optics. Opt Express 2012;20:A879-87.

[93] Arnaoutakis GE, Marques-Hueso J, Ivaturi A, Krämer KW, Mallick TK, Richards BS. Enhancement of Upconversion for Photovoltaics with β- NaYF4:Er3+ and Concentrating Integrated Optics. Proc Optical Nanostructures and Advanced Materials for Photovoltaics 2013; 2013 3-7 Nov; Tuscon, AZ, USA. p. 9-11.

[94] Ivaturi A, MacDougall SK, Martín-Rodríguez R, Quintanilla M, Marques-Hueso J, Krämer KW et al. Optimizing infrared to near infrared upconversion quantum yield of β-NaYF4:Er3+ in fluoropolymer matrix for photovoltaic devices. J Appl Phys 2013;114:013505.

[95] Shalav A, Richards B, Green M. Luminescent layers for enhanced silicon solar cell performance: up-conversion. Sol Energy Mater Sol Cells 2007;91:829-842.

[96] Goldschmidt JC, Fischer S, Löper P, Krämer KW, Biner D, Hermle M et al. Experimental analysis of upconversion with both coherent monochromatic irradiation and broad spectrum illumination. Sol Energy Mater Sol Cells 2011;95:1960-3.

[97] Fischer S, Frölich B, Steinkemper H, Krämer KW, Goldschmidt JC. Absolute upconversion quantum yield of β-$NaYF_4$ doped with Er^{3+} and external quantum efficiency of upconverter solar cell devices under broad-band excitation considering spectral mismatch corrections. Sol Energy Mater Sol Cells 2014;122:197-207.

[98] Fischer S, Favilla E, Tonelli M, Goldschmidt JC. Record efficient upconverter solar cell devices with optimized bifacial silicon solar cells and monocrystalline BaY_2F_8:30% Er^{3+} upconverter. Sol Energy Mater Sol Cells 2015;136:127-34.

[99] Chen YC, Chen TM. Improvement of conversion efficiency of silicon solar cells using up-conversion molybdate $La_2Mo_2O_9$:Yb, R (R=Er, Ho) phosphors. J Rare Earths 2011;29:723-6.

[100] de Wild-Scholten MJ. Energy payback time and carbon footprint of commercial photovoltaic systems. Sol Energy Mater Sol Cells 2013;119:296-305.

[101] Atre AC, Dionne JA. Realistic upconverter-enhanced solar cells with non-ideal absorption and recombination efficiencies. J Appl Phys 2011;110:034505.

[102] de Wild J, Meijerink A, Rath JK, van Sark WGJHM, Schropp REI. Towards upconversion for amorphous silicon solar cells. Sol Energy Mater Sol Cells 2010;94:1919-22.

[103] Qu B, Jiao Y, He S, Zhu Y, Liu P, Sun J et al. Improved performance of a-Si:H solar cell by using up-conversion phosphors. J Alloy Compd 2016;658:848-53.

[104] Chen Z, Zhang X, Zeng S, Liu Z, Ma Z, Dong G et al. Highly efficient up-conversion luminescence in $BaCl_2$:Er^{3+} phosphors via simultaneous multiwavelength excitation. Appl Phys Express 2015;8:032301.

[105] Chen Z, Jia H, Zhang X, Liu J, Zeng S, Li Y et al. $BaCl_2$:Er^{3+}—A High Efficient Upconversion Phosphor for Broadband Near-Infrared Photoresponsive Devices. J Am Ceram Soc 2015;98:2508-13.

[106] Chen Z, Wu G, Jia H, Sharafudeen K, Dai W, Zhang X et al. Improved Up-Conversion Luminescence from Er^{3+}:LaF_3 Nanocrystals Embedded in Oxyfluoride Glass Ceramics via Simultaneous Triwavelength Excitation. J Phys Chem C 2015;119:24056-61.

[107] Goldschmidt J, Löper P, Fischer S, Janz S, Peters M, Glunz SW et al. Advanced upconverter systems with spectral and geometric concentration for high upconversion efficiencies. Proc Conference on Optoelectronic and Microelectronic Materials and Devices; 2008 28 Jul-1 Aug; Sydney, Australia. p. 307-11.

[108] Fischer S, Ivaturi A, Fröhlich B, Rüdiger M, Richter A, Krämer KW et al. Upconverter Silicon Solar Cell Devices for Efficient Utilization of Sub-Band-Gap Photons Under Concentrated Solar Radiation. IEEE J Photovolt 2014;4:183-9.

[109] Arnaoutakis GE, Marques-Hueso J, Mallick TK, Richards BS. Coupling of sunlight into optical fibres and spectral dependence for solar energy applications. Sol Energy 2013;93:235-43.

[110] Arnaoutakis GE, Marques-Hueso J, Ivaturi A, Krämer KW, Fischer S, Goldschmidt JS et al. Enhanced up-conversion for photovoltaics via concentrating integrated optics. Opt Express 2014;22:A452-64.

[111] Arnaoutakis GE, Marques-Hueso J, Ivaturi A, Fischer S, Goldschmidt JS, Krämer KW et al. Enhanced energy conversion of up-conversion solar cells by the integration of compound parabolic concentrating optics. Sol Energy Mater Sol Cells 2015;140:217-23.

[112] Fischer S, Frölich B, Krämer KW, Goldschmidt JC. Relation between Excitation Power Density and Er3+ Doping Yielding the Highest Absolute Upconversion Quantum Yield. J Phys Chem C 2014;118:30106-14.

[113] Wang J, Ming T, Jin Z, Wang J, Song L, Yan C. Photon energy upconversion through thermal radiation with the power efficiency reaching 16%. Nat Commun 2014;5:5669.

[114] Boriskina SV, Chen G. Exceeding the solar cell Shockley–Queisser limit via thermal up-conversion of low-energy photons. Opt Commun 2014;314:71-8.

[115] Chen Z, Jia H, Sharafudeen K, Dai W, Liu Y, Dong G et al. Up-conversion luminescence from single vanadate through blackbody radiation harvesting broadband near-infrared photons for photovoltaic cells. J Alloy Compd 2016;663:204-10.

[116] O'Regan B, Grätzel M. Low cost and highly efficient solar cells based on the sensitization of colloidal titanium dioxide. Nat 1991;335:737-40.

[117] Wang Y. Recent research progress on polymer electrolytes for dye-sensitized solar cells. Sol Energy Mater Sol Cells 2009;93:1167-75.

[118] Wang ZS, Kawauchi H, Kashima T, Arakawa H. Significant influence of TiO_2 photoelectrode morphology on the energy conversion efficiency of N719 dye-sensitized solar cell. Coord Chem Rev 2004;248:1381-9.

[119] Shan GB, Demopoulos GP. Near-Infrared Sunlight Harvesting in Dye-Sensitized Solar Cells Via the Insertion of an Upconverter-TiO_2 Nanocomposite Layer. Adv Mater 2010;22:4373-77.

[120] Xie G, Lin J, Wu J, Lang Z, Li Q, Xiao Y et al. Application of upconversion luminescence in dye-sensitized solar cells. Chin Sci Bull 2011;56:96-101.

[121] Ramasamy P, Kim J. Combined plasmonic and upconversion rear reflector for efficient dye-efficient dye-sensitized solar cells. Chem Commun 2014;50:879-81

[122] Han G, Li D, Bai J, Diao G. Novel upconversion Er, Yb-CeO2 hollow spheres as scattering layer materials for efficient dye-sensitized solar cells. Sol Energy Mater Sol Cells 2017;160:54-9.

[123] Günes S, Neugebauer H, Sariciftci NS. Conjugated Polymer-Based Organic Solar Cells. Chem Rev 2007;107:1324-8.

[124] Wang H, Stubhan T, Osvet A, Litzov I, Brabec CJ. Up-conversion semiconducting MoO_3:Yb/Er nanocomposites as buffer layer in organic solar cells. Sol Energy Mater Sol Cells 2012;105:196-201.

[125] Damitha Adikaari AA, Etchart I, Guéring PH, Bérard M, Ravi S, Silva P et al. Near infrared up-conversion in organic photovoltaic devices using an efficient Yb^{3+}:Ho^{3+} Co-doped Ln_2BaZnO_5 (Ln = Y, Gd) phosphor. J Appl Phys 2012;111:094502.

[126] Chen W, Hou Y, Osvet A, Guo F, Kubis P, Batentschuk M et al. Sub-bandgap photon harvesting for organic solar cells via integrating up-conversion nanophosphors. Org Electron 2015;19:113-9.

[127] Zhao J, Ji S, Guo H. Triplet–triplet annihilation based upconversion: from triplet sensitizers and triplet acceptors to upconversion quantum yields. RSC Adv 2011;1:937-50.

[128] Schulze TF, Czolk J, Cheng YY, Fückel B, MacQueen RW, Khoury T et al. Efficiency Enhancement of Organic and Thin-Film Silicon Solar Cells with Photochemical Upconversion. J Phys Chem C 2012;116:22794-801.

[129] Robel I, Subramanian V, Kuno M, Kamat PV. Quantum dot solar cells. Harvesting light energy with CdSe nanocrystals molecularly linked to mesoscopic TiO_2 films. J Am Chem Soc 2006;128:2385-93.

[130] Wang K, Jiang J, Wan S, Zhai J. Upconversion enhancement of lanthanide-doped $NaYF_4$ for quantum dot-sensitized solar cells. Electrochimica Acta 2015;155:357-63.

[131] Ramachari D, Esparza D, López-Luke T, Romero VH, Perez-Mayen L, De la Rosa E et al. Synthesis of co-doped Yb^{3+}-Er^{3+}:ZrO_2 upconversion nanoparticles and their applications in enhanced photovoltaic properties of quantum dot sensitized solar cells. J Alloy Compd 2017;698:433-41.

[132] Kojima A, Teshima K, Shirai Y, Miyasaka T. Organometal Halide Perovskites as Visible-Light Sensitizers for Photovoltaic Cells. J Am Chem Soc 2009;131:6050-1.

[133] Mei A, Li X, Liu L, Ku Z, Liu T, Rong Y et al. A hole-conductor-free, fully printable mesoscopic perovskite solar cell with high stability. Sci 2014;345:295-8.

[134] Noh J, Seok S. Steps toward efficient inorganic–organic hybrid perovskite solar cells. MRS Bull 2015;40:648-53.

[135] Wang K, Jiang J, Wan S, Zhai J. Upconversion enhancement of lanthanide-doped $NaYF_4$ for quantum dot-sensitized solar cells. Electrochimica Acta 2015;155:362.

[136] Chen X, Hu W, Song H, Chen C, Xia H, Zhu Y et al. Highly Efficient LiYF4:Yb3+, Er3+ Upconversion Single Crystal under Solar Cell Spectrum Excitation and Photovoltaic Application. ACS Appl Mater Interfaces 2016;8:9071-9.

[137] He M, Pang X, Liu X, Jiang B, He Y, Snaith H et al. Monodisperse Dual-Functional Upconversion Nanoparticles Enabled Near-Infrared Organolead Halide Perovskite Solar Cells. Angew Chem Int Ed 2016;55:4280-4.

[138] Roh J, Yu H, Jang J. Hexagonal β-NaYF4:Yb^{3+}, Er^{3+} Nanoprism-Incorporated Upconverting Layer in Perovskite Solar Cells for Near-Infrared Sunlight Harvesting. ACS Appl Mater Interfaces 2016;8:19847-52.

[139] Wang H, Zhang Z, Qin J, Shi W, Liu Y, Gao H et al. Enhanced Photovoltaic Performance of Perovskite Solar Cells Based on Er-Yb Co-doped TiO2 Nanorod Arrays. Electrochimica Acta 2017;245:839-45.

[140] Huang X, Han S, Huang W, Liu X. Enhancing solar cell efficiency: the search for luminescent materials as spectral converters. Chem Soc Rev 2013;42:177.

[141] Huang X, Han S, Huang W, Liu X. Enhancing solar cell efficiency: the search for luminescent materials as spectral converters. Chem Soc Rev 2013;42:177.

[142] Huang X, Han S, Huang W, Liu X. Enhancing solar cell efficiency: the search for luminescent materials as spectral converters. Chem Soc Rev 2013;42:177.

[143] Judd BR. Optical Absorption Intensities of Rare-Earth Ions. Phys Rev 1962;127:750-61.

[144] García Sole J, Bausá LE, Jacque D. An Introduction to the Optical Spectroscopy of Inorganic Solids. Chichester: John Wiley & Sons Ltd; 2005. p. 207.

[145] Fischer S, Steinkemper H, Löper P, Hermle M, Goldschmidt JC. Modeling upconversion of erbium doped microcrystals based on experimentally determined Einstein coefficients. J Appl Phys 2012;111:013109.

[146] Shyichuk A, Câmara SS, Weber IT, Caneiro Neto AN, Nunes LAO, Lis S et al. Energy transfer upconversion dynamics in YVO_4:Yb^{3+}, Er^{3+}. J Lumin 2016:170:560-70.

[147] Govaerts YM, Verstraete MM. Raytran: a Monte Carlo ray-tracing model to compute light scattering in three-dimensional heterogeneous media. IEEE Trans Geosci Remote Sens 1998:36;493-505.

[148] Arnaoutakis GE, Marques-Hueso J, Ivaturi A, Krämer KW, Mallick TK, Richards BS. Enhancement of Upconversion for Photovoltaics with β- NaYF4:Er3+ and Concentrating Integrated Optics. Proc Optical Nanostructures and Advanced Materials for Photovoltaics 2013; 2013 3-7 Nov; Tuscon, AZ, USA. p. 11.

[149] Huang X, Han S, Huang W, Liu X. Enhancing solar cell efficiency: the search for luminescent materials as spectral converters. Chem Soc Rev 2013;42:185.

[150] Richards BS. Enhancing the performance of silicon solar cells via the application of passive luminescence conversion layers. Sol Energy Mater Sol Cells 2006;90:2333.

[151] Huang XY, Zhang QY. Near-infrared quantum cutting via cooperative energy transfer in Gd_2O_3:Bi^{3+}, Yb^{3+} phosphors. J Appl Phys 2009;105:053521.

[152] Wegh RT, Donker H, van Loef EVD, Oskam KD, Meijerink A. Quantum cutting through downconversion in rare-earth compounds. J Lumin 2000;87-9:1017-9.

[153] Fan B, Chlique C, Merdrignac-Conanec O, Zhang X, Fan X. Near-Infrared Quantum Cutting Material Er^{3+}/Yb^{3+} Doped La_2O_2S with an External Quantum Yield Higher than 100%. J Phys Chem C 2012;116:11652-7.

[154] C Strümpel, McCann M, Beaucarne G, Arkhipov V, Slaoui A, Švrček V et al. Modifying the solar spectrum to enhance silicon solar cell efficiency—An overview of available materials. Sol Energy Mater Sol Cells 2007;91:238–49.

[155] Richards BS, Shalav A. The role of polymers in the luminescence conversion of sunlight for enhanced solar cell performance. Synth Met 2005;154:61.

[156] Huang X, Han S, Huang W, Liu X. Enhancing solar cell efficiency: the search for luminescent materials as spectral converters. Chem Soc Rev 2013;42:185.

[157] Tai Y, Zheng G, Wang H, Bai J. Broadband down-conversion based near infrared quantum cutting in Eu^{2+}–Yb^{3+} co-doped $SrAl_2O_4$ for crystalline silicon solar cells. J Solid State Chem 2015;226:250-4.

[158] Boccolini A, Marques-Hueso J, Chen D, Richards BS. Physical performance limitations of luminescent down-conversion layers for photovoltaic applications. Sol Energy Mater Sol Cells 2014;122:8-14.

[159] Li Y, Wei X, Chen H, Pan Y, Ji Y. Near-infrared downconversion through host sensitized energy transfer in Yb^{3+}-doped $Na_2YMg_2(VO_4)_3$. Phys B 2015;478:95-8.

[160] de la Mora MB, Amelines-Sarria O, Monroy BM, Hernández-Pérez CD, Lugo JE. Materials for downconversion in solar cells: Perspectives and challenges. Sol Energy Mater Sol Cells 2017;165:59-71.

[161] Dumont L, Cardin J, Benzo P, Carrada M, Labbé C, Richard AL et al. D. C. SiN_x:Tb^{3+}–Yb^{3+}, an efficient down-conversion layer compatible with a silicon solar cell process. Sol Energy Mater Sol Cells 2016;145:84-92.

[162] González-Pérez S, Sanchiz J, González-Díaz B, Holinski S, Borchert D, Hernández-Rodríguez C et al. Luminescent polymeric film containing an Eu(III) complex acting as UV protector and down-converter for Si-based solar cells and modules. Surf Coat Technol 2015;271:106-11.

[163] Florêncio LA, Gómez-Malagón LA, Lima BC, Gomes ASL, Garcia JAM, Kassab LRP. Efficiency enhancement in solar cells using photon down-conversion in Tb/Yb-doped tellurite glass. Sol Energy Mater Sol Cells 2016;157:468-75.

[164] Yao N, Huang J, Fu K, Liu S, ED, Wang Y et al. Efficiency enhancement in dye-sensitized solar cells with down conversion material ZnO: Eu^{3+}, Dy^{3+}. J Power Sources 2014;267:405-10.

[165] Hou X, Xuan T, Sun H, Chen X, Li H, Pan L. High-performance perovskite solar cells by incorporating a $ZnGa_2O_4$:Eu^{3+} nanophosphor in the mesoporous TiO_2 layer. Sol Energy Mater Sol Cells 2016;149:121-7.

[166] Huang CK, Chen YC, Hung WB, Chen TM, Sun KW, Chang WL. Enhanced light harvesting of Si solar cells via luminescent down-shifting using $YVO_4:Bi^{3+}$, Eu^{3+} nanophosphors. Prog Photovolt Res Appl 2013;21:1507-13.

[167] Alonso-Álvarez D, Ross D, Klampaftis E, McIntosh KR, Jia S, Storiz P et al. Luminescent down-shifting experiment and modelling with multiple photovoltaic technologies. Prog Photovolt Res Appl 2015;23:479-97.

[168] Pi X, Li Q, Li D, Yang D. Spin-coating silicon-quantum-dot ink to improve solar cell efficiency. Sol Energy Mater Sol Cells 2011;95:2941-5.

[169] Huang X, Han S, Huang W, Liu X. Enhancing solar cell efficiency: the search for luminescent materials as spectral converters. Chem Soc Rev 2013;42:191-192.

[170] Rothemund R. Optical modelling of the external quantum efficiency of solar cells with luminescent down-shifting layers. Sol Energy Mater Sol Cells 2014;120:616–21.

[171] Lipovšek B, Solodovnyk A, Forberich K, Stern E, Brabec CJ, Krč J et al. Optical Model for Simulation and Optimization of Luminescent down-shifting Layers in Photovoltaics. Energy Procedia 2015;84:3-7.

[172] Lesyuk R, Marinov V, Hobbie EK, Elbaradei A, Tarnavchyk I, Bobitski Y. Toward cadmium-free spectral down-shifting converters for photovoltaic applications. Sol Energy Mater Sol Cells 2016;151:52-9.

[173] Hung WB, Chen TM. Efficiency enhancement of silicon solar cells through a downshifting and antireflective oxysulfide phosphor layer. Sol Energy Mater Sol Cells 2015;133:39–47.

[174] Ho WJ, Shen YT, Deng YJ, Yeh CW, Sue RS. Performance enhancement of planar silicon solar cells through utilization of two luminescent down-shifting Eu-doped phosphor species. Thin Solid Films 2016;618:141-5.

[175] Maalej O, Merigeon J, Boulard B, Girtan M. Visible to near-infrared down-shifting in Tm^{3+} doped fluoride glasses for solar cells efficiency enhancement. Opt Mater 2016;60:235-9.

[176] Raugei M, Bargigli S, Ulgiati S. Life cycle assessment and energy pay-back time of advanced photovoltaic modules: CdTe and CIS compared to poly-Si. Energy 2007;32:1310-8.

[177] Romeo N, Bosio A, Canevari V, Podestà A. Recent progress on CdTe/CdS thin film solar cells. Sol Energy 2004;77:795-801.

[178] Uekert T, Solodovnyk A, Ponomarenko S, Osvet A, Levchuk I, Gast J et al. Nanostructured organosilicon luminophores in highly efficient luminescent down-shifting layers for thin film photovoltaics. Sol Energy Mater Sol Cells 2016;155:1-8.

[179] Ross D, Alfonso-Álvarez D, Klampaftis E, Fritsche J, Bauer M, Debije MG et al. The Impact of Luminescent Down Shifting on the Performance of CdTe Photovoltaics: Impact of the Module Vintage. IEEE J Photovolt 2014;4:457-64.

[180] Hodgson SD, Brooks WSM, Clayton AJ, Kartopu G, Barrioz V, Irvine SJC. The impact of quantum dot concentration on the optical properties of QD/PMMA luminescent down-shifting films applied to CdTe photovoltaic devices. Nano Energy 2014;4:1-6.

[181] Song P, Zhang C, Zui P. Eu^{3+}-Mn^{2+}-doped bi-functional glasses with solar photon downshifting: Application to CdS/CdTe solar cells. J Alloy Compd 2016;661:14-9.

[182] Parel TS, Danos L, Markvart T. Application of concentrating luminescent down-shifting structures to CdS/CdTe solar cells with poor short wavelength response. Sol Energy Mater Sol Cells 2015;140:306-11.

[183] Goldschmidt J, Löper P, Fischer S, Janz S, Peters M, Glunz SW et al. Advanced upconverter systems with spectral and geometric concentration for high upconversion efficiencies. Proc Conference on Optoelectronic and Microelectronic Materials and Devices; 2008 28 Jul-1 Aug; Sydney, Australia. p. 309.

[184] Pan AC, del Cañizo C, Cánavos E, Santos NM, Leitão JP, Luque A. Enhancement of up-conversion efficiency by combining rare earth-doped phosphors with PbS quantum dots. Sol Energy Mater Sol Cells 2010;94:1923–6.

[185] Joannopoulos JD, Johnson SG, Winn JN, Meade RD. Photonic Crystals: Molding the Flow of Light. 2nd ed. Princeton: Princeton University Press; 2008.

[186] Marques-Hueso J, Peretti R, Arbargues R, Richards BS, Seassal C, Martínez-Pastor JP. Photovoltaics: Photonic Crystal-Driven Spectral Concentration for Upconversion Photovoltaics. Adv Opt Mater 2015;3:568-74.

[187] Boyer JC, van Veggel FCJM. Absolute quantum yield measurements of colloidal $NaYF_4$: Er^{3+}, Yb^{3+} upconverting nanoparticles. Nanoscale 2010;2:1417-9.

[188] Zou W, Visser C, Maduro JA, Pshenichnikov MS, Hummelen JC. Broadband dye-sensitized upconversion of near-infrared light. Nat Photonics 2012;6:560-4.

[189] Huang X. Broadband dye-sensitized upconversion: A promising new platform for future solar upconverter design. J Alloy Compd 2017;690:356-9.

[190] Sun L, Dong H, Zhang P, Yan C. Upconversion of rare Earth nanomaterials. Annu Rev Phys Chem 2015;66:629-31.

[191] Shao W, Chen G, Ohulchanskyy TY, Kazim A, Damasco J, Qiu H et al. Lanthanide-Doped Fluoride Core/Multishell Nanoparticles for Broadband Upconversion of Infrared Light. Adv Opt Mater 2015;3:575-82.

[192] Paudel HP, Zhong L, Bayat K, Baroughi MF, Smith S, Lin C et al. Enhancement of Near-Infrared-to-Visible Upconversion Luminescence Using Engineered Plasmonic Gold Surfaces. J Phys Chem C 2011;115-19028-36.

[193] Barnes WL, Dereux A, Ebbesen TW. Surface plasmon subwavelength optics. Nat 2003;424:824-30.

[194] Atre AC, García-Etxarri A, Alaeian H, Dionne JA. Toward high-efficiency solar upconversion with plasmonic nanostructures. J Opt 2012;14:024008.

[195] Liu Y, Xia Y, Jiang Y, Zhang M, Sun W, Zhao X. Coupling effects of Au-decorated core-shell β-$NaYF_4$:Er/Yb@SiO_2 microprisms in dye-sensitized solar cells: plasmon resonance versus upconversion. Electrochimica Acta 2015;180:394-400.

[196] Luoshan M, Bai L, Bu C, Liu X, Zhu Y, Guo K et al. Surface plasmon resonance enhanced multi-shell-modified upconversion $NaYF_4$:Yb^{3+}, Er^{3+}@SiO_2@Au@TiO_2 crystallites for dye-sensitized solar cells. J Power Sources 2016;307:468-73.

[197] Le KQ, John S. Synergistic plasmonic and photonic crystal light-trapping: Architectures for optical up-conversion in thin-film solar cells. Opt Express 2014;22:A1-12.

[198] Ahmed H, Doran J, McCormack SJ. Increased short-circuit current density and external quantum efficiency of silicon and dye sensitised solar cells through plasmonic luminescent down-shifting layers. Sol Energy 2016;126;146-55.

[199] Rüdiger M, Fischer S, Frank J, Ivaturi A, Richards BS, Kramer KW et al. Bifacial n-type silicon solar cells for upconversion applications. Sol Energy Mater Sol Cells 2014;128: 57-68.

[200] Kumar D, Verma K, Verma S, Chaudhary B, Som S, Sharma V et al. Recent advances in enhanced luminescence upconversion of lanthanide doped $NaYF_4$ phosphors. Sol Energy Mater Sol Cells. Forthcoming 2017.

[201] Favilla E, Cittadino A, Veronesi S, Tonelli M, Fischer S, Goldschmidt JC et al. Comparative analysis of upconversion efficiencies in fluoride materials for photovoltaic application. Sol Energy Mater Sol Cells 2016;157:415-21.

[202] Atwater JH, Spinelli P, Kosten E, Parsons J, Van Lare C, Van de Groep J et al. Microphotonic parabolic light directors fabricated by two-photon Lithography. Appl Phys Lett 2011;99:151113.

[203] Zhang Z, Zhang J, Chen N, Qu L. Graphene quantum dots: an emerging material for energy-related applications and beyond. Energy Environ Sci 2012;5:8869-90.

[204] Lee E, Ryu J, Jang J. Fabrication of graphene quantum dots via size selective precipitation and their application in upconversion-based DSSCs. Chem Commun 2013;49:9995-97.

[205] Schulze TF, Schmidt TW. Photochemical upconversion: present status and prospects for its application to solar energy conversion. Energy Environ Sci 2015;8:121.

[206] Wu TC, Congreve DN, Baldo MA. Solid State Photon Upconversion Utilizing Thermally Activated Delayed Fluorescence Molecules as Triplet Sensitizer. Appl Phys Lett 2015;107:031103.

[207] Yao N, Huang J, Fu K, Deng X, Ding M, Shao M et al. Enhanced light harvesting of dye-sensitized solar cells with up/down conversion materials. Electrochimica Acta 2015;154:273-7.

[208] Lee KT, Park JH, Kwon SJ, Kown HK, Kyhm J, Kwak KW et al. Simultaneous Enhancement of Upconversion and Downshifting Luminescence via Plasmonic Structure. Nano Lett 2015;15:2491-97.

[209] Loiko PA, Khaidukov NM, Méndez-Ramos J, Vilejshikova EV, Skoptsov NA, Yumashev KV. Up- and down-conversion emissions from Er^{3+} doped K_2YF_5 and K_2YbF_5 crystals. J Lumin 2016;170:1-7.

[210] Bahadur A, Yadav RS, Yadav RV, Rai SB. Multimodal emissions from Tb^{3+}/Yb^{3+} co-doped lithium borate glass: Upconversion, downshifting and quantum cutting. J Solid State Chem 2017;246:81-6.

[211] Wang Y, Zhang H, Qu S, Su C. Downconversion and upconversion emissions of $GdPO_4:Yb^{3+}/Tb^{3+}$ and its potential applications in solar cells. J Alloy and Compd 2016;677:266-70.

[212] Aarts L, van der Ende BM, Meijerink A. Downconversion for solar cells in $NaYF_4$:Er,Yb. J Appl Phys 2009;106:023522.

[213] European Commission, Community Research and Development Information Service. Final Report - EPHOCELL Smart light collecting system for the efficiency enhancement of solar cells. Terrassa (Spain): Acondicionamiento Tarrasense Associacion (LEITAT); 2013 Mar. Project ID: 227127. Funded under: FP7-ENERGY.

[214] Ross D, Alfonso-Álvarez D, Klampaftis E, Fritsche J, Bauer M, Debije MG et al. The Impact of Luminescent Down Shifting on the Performance of CdTe Photovoltaics: Impact of the Module Vintage. IEEE J Photovolt 2014;4:463.

[215] Le Donne A, Acciarri M, Narducci D, Marchionna S, Binetti S. Encapsulating Eu^{3+} complex doped layers to improve Si-based solar cell efficiency. Prog Photovolt Res Appl 2009;17:519–25.

[216] Humphries M. Rare Earth Elements: The Global Supply Chain. Washington DC (USA): Congressional Research Service; 2013 Dec. Report No.: R41347.

[217] Rüdiger M, Fischer S, Frank J, Ivaturi A, Richards BS, Kramer KW et al. Bifacial n-type silicon solar cells for upconversion applications. Sol Energy Mater Sol Cells 2014;128:67.

[218] Semonin OE, Luther JM, Choi S, Chen HY, Gao J, Nozik AJ et al. Peak external photocurrent quantum efficiency exceeding 100% via MEG in a quantum dot solar cell. Sci 2011;334:1530-3.

[219] Shpaisman H, Niitsoo O, Lubomirsky I, Cahen D. Can up- and down-conversion and multi-exciton generation improve photovoltaics? Sol Energy Mater Sol Cells 2008;92:141-6.

- Solar cell efficiency enhanced up to 70% relative by converting incident spectrum
- Range of cell technologies attain greater performance at short and long wavelengths
- 35 fold increase in short circuit current density enhancement from 2011-15
- Further potential from optics and nanostructures which are independently optimized
- Cost per watt could be reduced by €0.06 and economic analysis of up-to-date results

Technology	Maximum efficiency (%)	Cost per W_p ($)
Silicon (monocrystalline)	25.0	1.10-1.40
Silicon (multi-crystalline)	21.3	0.80-0.90
Silicon (amorphous)	13.6	0.45-0.53
Copper Indium Gallium Selenide	22.1	0.55-0.65
Cadmium Telluride	22.1	0.50-0.60
Dye Sensitized	11.9	0.25-0.40
Perovskite	22.1	0.20-0.30
Concentrator Multijunction	46.0	1.50-2.30

UC material	$\lambda_{excitation}$ (nm)	$\lambda_{emission}$ (nm)	Solar cell	Device response	Ref.
Er^{3+} doped $NaYF_4$	1460-1600	980	c-Si	+0.69 mA/cm^2 J_{SC} under 732 suns	103
Er^{3+} doped $NaYF_4$	1450-1600	980	c-Si	+4.03 mA/cm^2 J_{SC} under 77 suns	104
Er^{3+} doped $NaYF_4$	1450-1600	980, 805, 655, 540	c-Si	+13.1 mA/cm^2 J_{SC} under 210 suns	115
Er^{3+} doped BaY_2F_8	1493	1000	c-Si	+17.2 mA/cm^2 J_{SC} under 95 suns	105
Er^{3+} doped $NaYF_4$	1523	980	c-Si	1.33% EQE (without optic) and 1.80% EQE (with optic) under 0.024 W/cm^2 laser	118
Er^{3+} doped $BaCl_2$	808, 980	667, 546, 530, 496, 455, 410	a-Si:H	+0.6 mA/cm^2 J_{SC} under bi-wavelength 70 and 100 mW lasers	112
Er^{3+} doped LaF_3 in oxyfluoride ceramic	808, 980, 1530	657, 542	a-Si:H	+1.7 mA/cm^2 J_{SC} under tri-wavelength 1400, 1200 and 800 W/cm^2 lasers	113
$CeVO_4$ via thermal UC	1064, 980, 808	750-700	a-Si:H	+0.91 mA/cm^2 J_{SC} under 831 W/cm^2	124
Yb^{3+} - Er^{3+} co-doped $NaYF_4$	980	650, 536, 518	a-Si:H	+1.74 mA/cm^2 J_{SC} and +0.41% PCE under AM 1.5G	110

Yb^{3+} -Er^{3+} co-doped TiO_2	980	700-510	DSSC	+0.87% PCE under AM 1.5	129
Yb^{3+} - Er^{3+} co-doped CeO_2	980	525-680	DSSC	+1.54% PCE under AM 1.5	131
Yb^{3+} - Er^{3+} co-doped $NaYF_4$	975	655, 540	OSC	+0.46% PCE under AM 1.5 G	135
Tm^{3+} - Yb^{3+} - Er^{3+} co-doped $NaYF_4$	980	650, 540, 520, 475, 400	QDSC	+2.15 mA/cm^2 J_{SC} +0.73% PCE (+17.6% and 20% relative increases) under AM 1.5 G	139
Yb^{3+} -Er^{3+} co-doped ZrO_2	970	725-500	QDSC	+1.06% PCE (+55% relative increase) under 0.1 W/cm^2	140
Yb^{3+} - Er^{3+} co-doped $LiYF_4$	1540, 980	700-500	PSC	+0.87% PCE (+7.9% relative increase) under 7-8 suns	145
Yb^{3+} - Er^{3+} co-doped $NaYF_4$	980	655, 543, 523, 408	PSC	+1.9% PCE (+13.7% relative increase) under AM 1.5 G	147
Yb^{3+} -Er^{3+} co-doped TiO_2 nanorod arrays	980	512-680	PSC	+2.6% PCE (+20.8% relative increase) under AM 1.5 G	148

DC material	$\lambda_{excitation}$ (nm)	$\lambda_{emission}$ (nm)	Solar cell	Device response	Ref.
Eu^{3+} in silicon nitride matrix	325	980	c-Si	N/A	161
Eu^{3+} containing aromatic complex in PMMA	250-360	665	c-Si	+5.8% EQE under 100W Xe lamp	162
Tb^{3+} - Yb^{3+} co-doped tellurite glass	355, 482	548, 980	c-Si	+7% relative PCE under 0.1W/cm^2	163
Eu^{3+} - Dy^{3+} co-doped ZnO (alongside graphene loading)	338, 394	394, 458, 483, 575, 593, 611	DSSC	+6.06 mA/cm^2 and +3.18% PCE (212% and 245% relative increases) under 0.1W/cm^2	164
Eu^{3+} doped $ZnGa_2O_4$	380-500	450-720	PSC	+3.48 mA/cm^2 and +3.67% PCE (17.2% and 34.4% relative increases) under AM 1.5 G	165

LDS material	$\lambda_{excitation}$ (nm)	$\lambda_{emission}$ (nm)	Solar cell	Device response	Ref.
Eu^{3+} doped Gd_2O_2S	200-350	624	mc-Si	+6.47 mA/cm^2 and +2.67% PCE under 1 sun	173
Eu^{2+} doped phosphors in SiO_2	250-360	512, 610	c-Si	+19.85% J_{SC} and +16% relative PCE under AM 1.5 G	174
Tm^{3+} doped fluoride glass	355, 482	548, 980	c-Si	+1.4% relative PCE under AM 1.5 G	175
Organosilicon lumiphores in EVA or PMMA	375	575	CIGS	+54% EQE at 360nm and +4.3% relative PCE under AM 1.5 G	178
Organic dyes in EVA and FEP	375, 475, 500, 520	425, 525, 560, 575	CdTe	+5.3% and +9.7% J_{SC} under 1.5 AM G	179
QDs in PMMA	300-500	540	CdTe	+1.7% PCE under AM 1.5 G	180
Mn^{2+} - Eu^{3+} doped phosphate glass	392	615	CdTe	+7.14% relative PCE under 0.1 W/cm^2	181

Dyes in PMMA	425-475	500-650	CdTe	+5% relative J_{SC} (non-concentrating) and up to +20% relative J_{SC} (concentrating) under 300 W Xenon lamp	182

Rare earth ion	Process	ΔPCE relative (%)	Solar cell	Maximum mass of ion to reduce cost per watt (mg/W)	Ref.
Eu^{3+}	UC	20.8	PSC	0.16	161
Eu^{3+}	DC	34.4	PSC	0.06	162
Tb^{3+} - Yb^{3+}	LDS	16.0	c-Si	0.15	163
Eu^{3+} - Dy^{3+}	UC/DC	70.0	DSSC	0.44	164